ECG Artefact Suppression and External Data Synchronization with the Medtronic Percept, a Deep Brain Stimulator with Sensing Technology

M.J. Stam

TU Delft

ECG Artefact Suppression and External Data Synchronization with the Medtronic Percept, a Deep Brain Stimulator with Sensing Technology

By
Mariëlle Jacquelien Stam

to obtain the degree of Master of Science
in Biomedical Engineering at the Delft University of Technology,
to be defended publicly on Wednesday June 30, 2021 at 10:00 AM

Student Number:	4953673	
Project Duration:	September 1, 2020 - June 30, 2021	
Thesis Committee:	Schouten, Dr.ir A.C.	Supervisor TU Delft
	Beudel, Dr. M.	Supervisor Amsterdam UMC
	Van der Helm, Prof.dr. F.C.T.	TU Delft

Delft University of Technology
Faculty of 3mE
Mekelweg 2
2628 CD Delft

This thesis will not be made publicly available until June 30, 2023

Acknowledgements

Before submitting my thesis I would like to take the time to thank a few people that helped me in my process towards graduation. The same result would not have been possible to achieve without their contributions.

First of all, many thanks to the NeuroMuscular Control Lab headed by Alfred Schouten and Winfred Mugge for their guidance throughout my graduation project. The lab has been a place of advice and feedback, but also felt like a meeting point or a small community through the biweekly (virtual) meetings in times of corona. Special thanks to Alfred for your supervision and mentorship throughout numerous Teams-calls and meetings. Your sharp eye for detail have triggered me to continuously improve the report. Thanks for teaching me so much about being a researcher. It will prove of great help for my future (academic) career.

I would like to thank the Percept Research Group at the Amsterdam UMC, in particular my supervisor Martijn Beudel. Thank you Martijn, for facilitating this project, for your trust and support, and for giving me the opportunity to experience the motivating environment of the University of Oxford where I had my first amazing glimpse into the world of science. Special thanks to both Arthur and Dan, for being a warm welcome at the department, for sharing your knowledge with me and for always standing by, both literally and figuratively, during patient recordings and online. Finally, thanks to Pallas, for exchanging ideas and providing mental support.

To all the people I have met during my time at the TU, thank you for welcoming me with open arms and for switching off my mind during the essential coffee breaks and social drinks. You have really made my experience in Delft complete.

Finally, to my parents, sister and friends, thanks so much for your endless support throughout my years of study. You have always motivated me to get the most out of it, and I can confidently say I did.

Preface

This thesis titled "ECG Artefact Suppression and External Data Synchronization with the Medtronic Percept, a Deep Brain Stimulator with Sensing Technology" is submitted in partial fulfilment of the requirements for the degree of Master of Science at the Delft University of Technology, Netherlands. This study was conducted under the joint supervision of Dr.ir. A.C. Schouten in the Department of BioMechanical Engineering at the Faculty of Mechanical, Maritime and Materials Engineering and Dr. M. Beudel in the Department of Neurology at the Amsterdam UMC. Despite the outbreak of coronavirus disease 2019 (COVID-19), it was still allowed to collect data from patients at the hospital. These were the first measurements at the Amsterdam UMC using the first and only commercially available sensing technology in deep brain stimulation: the Medtronic Percept™. Apart from the patient recordings, all remaining work of the project had to be done at home. This did not only challenge my discipline, but also challenged me to work independently and to pro-actively reach out to knowledgeable individuals. This work is to the best of my knowledge original, except where acknowledgments and references are made to previous work.

Abbreviations

ECG	Electrocardiograph
DBS	Deep Brain Stimulation
PD	Parkinson's Disease
ET	Essential Tremor
DYS	Dystonia
IPG	Implanted Pulse Generator
STN	Subthalamic Nucleus
VIM	Nucleus Ventralis Intermedius
GPi	Globus Pallidus internus
LFPs	Local Field Potentials
EMG	Electromyography
CMRR	Common Mode Rejection Ratio
PSD	Power Spectral Density
ICA	Independent Component Analysis
ch	channel
pt	patient
STD	Standard Deviation

Contents

Acknowledgements i

Preface ii

Abbreviations iii

Report

1. Introduction **1**

2. Methods **2**
2.1 Participants 2
2.2 Percept Data Collection 3
2.3 TMSi Data Collection 3
2.4 ECG Artefact Removal 4
2.5 Synchronization 5

3. Results **6**
3.1 Stimulation Artefact 6
3.2 ECG Artefact Removal 7
3.3 Synchronization 9
3.4 Proof of Concept for Tasks Analysis 11

4. Discussion **12**

5. Recommendations **14**

6. Conclusion **15**

References **15**

Appendices

ECG Artefact Suppression and External Data Synchronization with the Medtronic Percept, a Deep Brain Stimulator with Sensing Technology

Mariëlle J Stam[1]

[1] *Neuro Muscular Control Lab, BioMechanical Engineering, Delft University of Technology, Mekelweg 2, 2628 CD, Delft, The Netherlands*

Abstract— Deep brain stimulation (DBS) is used to treat a variety of movement disorders. In current DBS therapy, the stimulation parameters are manually adjusted based on a subjective assessment of patient's symptoms. State-of-the-art DBS research focuses on recording brain activity to create a patient-specific neuronal profile that correlates with the patient's symptom-severity. The neuronal profile could then be used as feedback signal for an adaptive DBS system that automatically adjusts the stimulation. The Medtronic Percept™ is the first commercially available, fully implanted neurostimulator with sensing technology. In this study, the neuronal activity in the form of local field potentials (LFPs) of eleven patients were recorded with Percept during both stimulation off- and on. To obtain a reliable neuronal profile from the LFPs, the signals should be free from electrocardiography (ECG) artefact and should be synchronized with externally recorded data that informs us about the patient's symptom-severity. A template subtraction method and a method based on independent component analysis were developed to suppress ECG artefact. Both methods were compared to the ECG removal method of the Perceive Toolbox. Three methods of synchronization were explored: externally tapping, using the stimulation artefact, and by ECG cross-correlation. Results show the template subtraction method to most effectively suppress ECG artefacts while preserving LFP frequency content. To save effort but assure accuracy of the synchronization, the ECG cross-correlation method should be applied though validated by confirming accurate alignment of the stimulation artefact. The development and evaluation of the ECG artefact suppression- and external data synchronization methods contribute to research focused on finding a reliable feedback signal for adaptive DBS.

Index Terms—DBS, Movement Disorders, Medtronic Percept, ECG Artefact, Synchronization.

1 Introduction

Deep brain stimulation (DBS) is an important therapeutic strategy for a variety of movement disorders, such as Parkinson's Disease (PD), Essential Tremor (ET), and Dystonia (DYS). Patients are implanted with a DBS system when medication have become less effective or when side effects of the medicines interfere with daily activities. To date, over 160,000 patients worldwide are treated with DBS [1]. Electrical current is generated by an implanted pulse generator (IPG) and is targeted to structures in the basal ganglia through implanted electrodes [2]. Although the underlying principles and exact mechanisms of DBS are not fully understood, the electrical current is intended to regulate pathological activity in the deep brain structures. In PD, the electrodes are generally implanted in the subthalamic nucleus (STN). The nucleus ventralis intermedius (VIM) of the thalamus is a popular target for DBS in ET and the internal segment of the globus pallidus (GPi) is usually implanted in DYS.

Current DBS therapy requires a clinician to manually adjust the stimulation parameters (frequency, amplitude, pulse width) based on a subjective assessment of the patient's symptoms. Adjusting the parameters is an ad hoc empirical process which is expensive in terms of time, price and most importantly, patient discomfort [3]. There is quite a big variation of clinical outcomes between patients [4] and DBS frequently causes unwanted side effects [5].

Considering the limitations of current neurostimulation, state-of-the-art DBS research aims to develop adaptive neurostimulation that makes the parameter adjustments by a clinician unnecessary. Whereas conventional DBS delivers continuous stimulation, an adaptive DBS system actively adjusts stimulation to meet the real-time patient needs. Adaptive DBS limits DBS-induced side effects [6], [7] and saves energy, therefore prolongs battery lifetime and reduces IPG replacement surgeries [8].

A critical determinant of the performance of adaptive DBS is the reliability of the feedback signal. In order to meet the real-time patient needs, the feedback signal should be indicative of the patient's clinical state. In current adaptive DBS research, the feedback signal is recorded from the basal ganglia structures in the form of local field potentials (LFPs). LFPs are measured as a differential signal between the two contacts adjacent to the stimulation contact on the implanted electrode lead [9]. These LFPs show oscillations at several frequency bands, including the delta and theta band (1 $\sim$ 7 Hz), alpha and beta band (8 - 35 Hz), gamma band (35 - 200 Hz) and high frequency oscillations ($>$ 200 Hz). Parkinsonian motor symptoms (rigidity and bradykinesia) are found to worsen with increased beta activity amplitude [10]. Similarly, a correlation is also found between a treatment-induced reduction of beta activity and an improvement of bradykinesia-rigidity [7], [11], [12]. Dyskinesia symptoms are reported to be linked to an

increased amplitude of LFPs at low theta/alpha frequencies (4 - 8 Hz) [13] and tremor to potentials at tremor frequency (4 - 7 Hz) [14]. With the intention to develop a reliable feedback signal, adaptive DBS research explores the ability of this disease-specific pathological brain activity to monitor therapeutic demand.

The initial studies to adaptive DBS recorded the basal ganglia LFPs via externalized electrode leads between operations for electrode placement and IPG implantation [9], [15], [16]. For these recordings, external customized neurostimulators were used. Only recently, a fully implanted neurostimulator able to simultaneously record the LFPs and deliver stimulation is commercially available: the Medtronic Percept™. The LFPs are stored on the Percept and can be viewed real time on the tablet programmer. This data can also be exported wirelessly for offline data processing.

1.1 Problem Statement

Since recording LFPs with a fully implanted DBS system is such a novel technique, there is only limited knowledge of the artefacts that may corrupt the recorded signals. Nevertheless, the heart as strongest source of electrical activity in the human body causes an electrocardiography (ECG) artefact in all types of biomedical signals. Surface electromyography (EMG) recordings of the trunk muscles, for example, are often contaminated by ECG [17], [18], [19]. As a matter of fact, the neurostimulator is generally implanted in the chest or abdomen, so in close proximity of this large signal generator. The ECG signals are in the range of 0.5 mV to 5 mV [20], whereas the LFP signals are in the range of 1 - 20 μV. The ECG artefact is superimposed on top of the LFPs and is difficult to filter, due to considerable overlapping of the frequency spectra of the signals [21].

The ECG artefact can be attributed to an inadequate common mode rejection ratio (CMRR) of the sensing input chain of the neurostimulator. As LFPs are measured as a differential signal, the ECG spikes are regarded as common mode signals which can be rejected by differentiating [22]. Studies have shown that a CMRR greater than 60 dB is required to eliminate ECG artefacts [23]. However, due to limited power consumption and size of the neurostimulator, it is challenging to achieve a high CMRR in an implantable system. Additionally, slight leakage of fluid into the IPG can lead to an input impedance mismatch. Such mismatch breaks the symmetry of the differentiated signal, which alters the CMRR [24].

Apart from the ECG artefact contaminating the LFPs, another challenge for offline data processing is the fact that the LFPs are isolated from other possible data inputs. However, in order to explore the ability of the LFPs to serve as a reliable feedback signal for adaptive DBS, they should be indicative of the patient's clinical state. Externally recorded data, such as accelerometry, can inform us about the patient's symptom-severity [25], [26]. Correlating this data with the recorded LFPs will result in a patient-specific profile of neuronal activity that is associated with the presence and severity of the symptoms. Before such patient-specific profile can be obtained, the externally recorded data should be synchronized with the LFPs recorded with the Percept.

1.2 Goal

To obtain a reliable patient-specific neuronal profile, the ECG artefact in the LFPs should be mitigated. Some research focuses on reducing sensing sensitivity to cardiac artefacts by exploring the effect of neurostimulator placement [22], [23]. However, to also obtain reliable LFP signals from already implanted systems, the first goal of this study is to remove the ECG artefact at the stage of signal processing. To be able to correlate the cleaned LFPs to the patient's symptom-severity, the second goal of this study is to synchronize the LFPs stored on the Percept with externally recorded data.

2 Methods

2.1 Participants

Eleven patients participated in this study: two patients suffering from Dystonia, one Essential Tremor patient, and eight patients suffering from Parkinson's Disease (Table 1). All patients were bilaterally implanted (one electrode lead per hemisphere) between 2013-2016. Due to battery depletion of their old IPG, the patients received the Medtronic Percept™ neurostimulator between September 2020 and March 2021. To reduce the patient burden, all recordings were performed immediate post-operative, right after the Percept was placed. Each recording took between 20-30 minutes during which the patient was asked to perform a behavioural protocol twice, first while the stimulation was off (off-DBS) and then while the stimulation was on (on-DBS). The protocol included a period of rest, a part of reading out loud and a variety of upper limb movements. During the recordings, patients lay comfortably on a bed with the head rest in a 45 degree angle and were instructed not to talk or sleep (Fig. 1). The study was approved by the local ethics committee of the Amsterdam UMC – Academic Medical Center and informed written consent was received from all patients.

Fig. 1: Schematic overview of the experimental setup. On the left the wireless communication via a relay device between the implanted Percept and the tablet programmer. On the right the external data running through the TMSi amplifier to the laptop. A webcam videotaped the recording.

Table 1. Information of patients' DBS therapy

n	Disease	Year of Electrode Implantation	Brain Target	Site of Percept	Stimulation Parameters (L / R)			
					Stimulation Contact	Frequency (Hz)	Pulse Width (µs)	Amplitude (mA)
1	DY	2014	GPi	Chest Right	1 / 1	130 / 130	60 / 60	2.0 / 2.4
2	DY	2015	GPi	Chest Left	1 / 1	180 / 180	90 / 90	5.4 / 5.2
3	ET	2014	Vim	Chest Right	1 / 1	130 / 130	60 / 60	1.4 / 1.2
4	PD	2014	STN	Chest Right	1 / 2	130 / 130	60 / 60	2.5 / 2.6
5	PD	2013	STN	Chest Right	1 / 1	130 / 130	60 / 60	1.8 / 2.7
6	PD	2016	STN	Chest Right	1 / 2	130 / 130	60 / 60	1.6 / 3.7
7	PD	2013	STN	Chest Left	1 / 2	180 / 180	90 / 60	2.1 / 2.7
8	PD	2013	STN	Chest Left	1+2 / 2	80 / 80	60 / 60	1.6 / 1.5
9	PD	2015	STN	Chest Right	1 /1	125 / 125	60 / 60	2.2 / 2.6
10	PD	2015	STN	Abdomen Right	1 / 2	130 / 130	60 / 60	2.8 / 2.6
11	PD	2015	STN	Chest Right	1 /1	125 / 125	60 / 60	2.3 / 3.5

2.2 Percept Data Collection

In all patients, LFPs were recorded from both electrode leads. To enable simultaneous stimulation and sensing in the on-DBS condition, the manufacturer of the Percept has put a lot of effort into avoiding the artefact caused by stimulation. These include (1) the use of a common mode rejection to suppress such stimulation artefact by "sandwiching" the monopolar electrode(s) between the two differential sensing electrodes. In monopolar stimulation configuration, the titanium case of the Percept acts as the return electrode (anode). In electrical terms, this is an infinite distance away from the neuronal elements that are stimulated and can therefore be considered monopolar stimulation. All patients were implanted with the Medtronic leads 3389 model, which contains four electrode contacts. Therefore, monopolar stimulation could be applied through either or both of the two middle contacts. It depended on the patients' pre-operative DBS settings which contact(s) was/were used for stimulation (Table 1). According to the stimulation contact(s), contact pair 0-2, 0-3, or 1-3 was used for the bipolar recording of the LFPs. To maintain consistency, the same sensing pair was used in both the off- as well as on-DBS condition.

Another technique to avoid stimulation artefact is (2) preventing sense channel saturation by rejecting the stimulation artefact prior to amplification. Additionally, (3) adding a high pass filter that removes the DC content in the time domain prior to performing the Fast Fourier transform as part of the frequency analysis helps to reduce the transient response to stimulation ramps. To help mitigate the stimulation artefact further, (4) the stimulation pulse is applied with an active recharge to achieve charge balance in a short time interval (100 μs), instead of the full passive recharge duration (10 ms). In fact, optimizing the active recharge ratio allows to limit the peak to peak input into the sensing channel and avoid amplifier saturation. By minimizing stimulation peaks, the residual voltage on the electrode coupling capacitor approaches zero, which improves the step response that occurs when the stimulation parameters are adjusted. This is important for control algorithms that require fast turn-on and turn-off times.

The sampling rate of the Percept is 250 Hz. By default, the Percept has two low pass filters of 100 Hz and one 1 Hz high pass filter, which is configurable up to 10 Hz. The raw LFPs were gained up by 250x, buffered on the device, and streamed wirelessly to the Percept tablet programmer. This data was exported as JSON-file and visualized offline using the open-source Perceive Toolbox (www.github.com/neuromodulation/perceive/) and the FieldTrip Toolbox for EEG/MEG-analysis ([27], http://fieldtriptoolbox.org) in Matlab (version R2020b, The Mathworks, Inc.,Natick, MA, USA).

2.3 TMSi Data Collection

Two 3D accerelometers ($\pm$ 3g, TMS International, The Netherlands) were attached to the dorsal surface of the right and left hand in order to measure kinematic

movements of the hand and the presence of tremor. A bipolar ECG signal was measured between two electrodes placed on the right and left shoulder. Two electrodes were placed on the head at the F3 and F4 positions of the 10-20 electroencephalography placement system to capture the electrical signal of the DBS. The patient ground was placed on cervical C7 vertebrae. The data was recorded using a TMSi Porti amplifier (monopolar, average reference, anti-aliasing low-pass filtering with a cut-off frequency of 500 Hz and sampling frequency of 2048Hz, TMSi, The Netherlands).

The software application toolbox TMSi Polybench was used to monitor the recording. Triggers were manually pressed on the Polybench software to indicate the start and stop of each task of the protocol and an USB Webcam (Trust Exis) was connected to videotape the recording. A schematic overview of the complete experimental setup is visualized in Fig. 1.

All data running through the TMSi amplifier was also imported into Matlab and analyzed using FieldTrip. This data was band stop (Notch) filtered for the power-line interference (between 49-51 Hz) and its harmonics (99-101 Hz).

2.4 ECG Artefact Removal

The LFP signals that contain an ECG artefact will be presented both in time- as well as frequency domain. The frequency domain analysis is done by evaluating the mean relative power spectral density (PSD). Relative rather than absolute PSD is analysed in order to aggregate the results of different participants. Also, absolute power is more likely to be dependent on proximity to the LFP source than relative power and to vary with minor changes in recording technique [28]. The relative PSD parameter gives an indication of the feasibility of the LFPs to serve as a feedback signal for adaptive DBS.

First, the absolute PSD is estimated by Welch's method, using an Hanning window for overlapping segments. The duration of the recordings is between 7.5-14.5 minutes. Segments of four seconds (1000 samples) with 50% overlap are used. The relative PSD is obtained by normalizing the power spectrum to the summed average power of 0.5-45 and 55-95 Hz [29]. The 0–0.5 and 45–55 Hz ranges are omitted so as to avoid contamination by movement artefact and mains noise, respectively. Only the relative PSD up to 35 Hz will be shown, since these are the most interesting frequencies for the patient cohorts in the current study.

Common methods used to remove ECG artefact require a multi-channel recording or an ECG reference signal. The LFP signal is a single-channel recording, usually independently recorded without ECG reference. Most existing methods can therefore not directly be applied to the LFP signals. During the course of the current thesis project, the open-source Perceive Toolbox was extended with a method to remove ECG artefact from the brain recordings. The Perceive ECG removal method applies cross-correlation over sliding windows to create a recording-specific template of the ECG artefact. It then uses pattern matching (correlation) of the template on the raw signal to identify segments of the signal affected by the ECG artefact. These segments are replaced by mirrored padding. For the current project, two other methods to remove ECG artefact from the LFP data are proposed: 1) a template subtraction method and 2) an approach based on independent component analysis (ICA). The flow charts of the methods are shown in Fig. 2. The template subtraction is proposed because it is a traditional ECG removal method [30], whereas the ICA-based method is a fairly new and unexplored approach to remove ECG

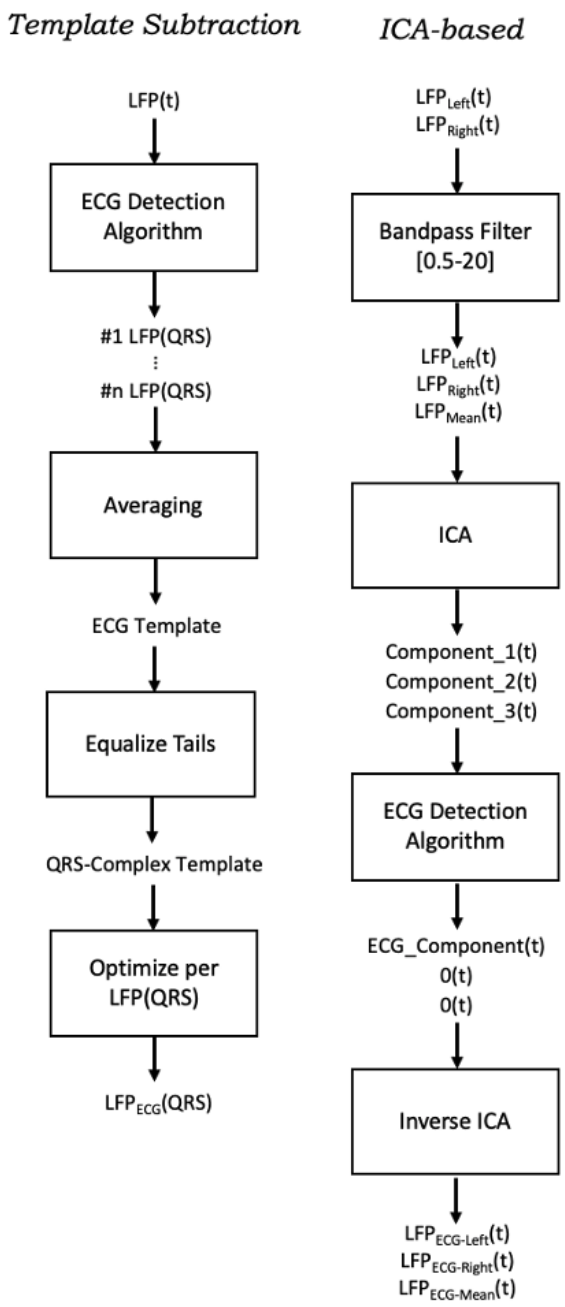

Fig. 2: Flow charts of template subtraction and ICA-based ECG removal methods. For both charts, the output is the ECG artefact which is subtracted from the original LFP signal, as described in (2) and (4).

artefact from biomedical signals [19]. Despite its novelty, studies using electroencephalography (EEG) and magnetoencephalography (MEG) have showed an improved signal quality and allowed better clinical interpretation after ICA-based ECG removal [31], [32], [33], [34].

2.4.1 Template Subtraction

The first step of the template subtraction method is to create a recording-specific QRS complex template. The QRS complex is the most prominent repeating peak in the ECG signal and corresponds to the depolarization of the right and left ventricles of the heart. The LFP signal is normalized and applied with an ECG-detection algorithm that searches for R-peaks with a specific height (at least twice the standard deviation) and at a specific distance apart (500 ms). The algorithm accounts for a negative QRS complex. LFP signals containing at least one R-peak every three seconds and a heart rate of at least 40 beats per minute were specified as contaminated with the ECG artefact. These criteria are included because they led to the most accurate automatic detection of ECG artefact for the current set of LFP signals. Of the signals specified as containing ECG artefact, epochs of 400 ms around the R-peaks (50 samples before and after) are made (QRS complex epochs) and are averaged to create the recording-specific ECG artefact template. The part of this template that contains the QRS complex is kept and the tail values are set equal (preferably zero).

On each QRS complex epoch in the original LFP signal, *LFP(QRS)*, the QRS complex template is optimized by adjusting the parameters, *scale* and *offset*, such that the sum of squared error is minimized (1):

$$LFP_{ECG}(QRS) = scale(QRS) * QRS_{template} + offset(QRS) \quad (1)$$

This QRS-specific optimized template, $LFP_{ECG}(QRS)$, is then subtracted from the QRS complex epoch in the original LFP signal, *LFP(QRS)*, to obtain the LFP signal at the QRS complex epochs without ECG artefact: $LFP_{clean}(QRS)$ (2):

$$LFP_{clean}(QRS) = LFP(QRS) - LFP_{ECG}(QRS) \quad (2)$$

2.4.2 Independent Component Analyis

ICA is a method for solving the Blind Source Separation problem by assuming that the different source signals are statistically independent. Independence means that observing the value of one source signal does not give any information about the value of another source signal. The goal of ICA is then to determine the source signals given only the observed mixtures. This model can be put into a mathematical equation by:

$$LFP(t) = MixingMatrix * Sources(t) \quad (3)$$

where *LFP* contains the measured (mixed) signals, which are obtained by multiplying the vector of independent source signals, *Sources*, by a specific *Mixing Matrix*.

Whereas the template subtraction method is applied to each individual sensing channel, ICA can only be applied to multi-channel recordings [35]. The multidimensional input for ICA is obtained by using the LFP signals of both the left- and right hemisphere of the patient, as well as the mean of these two signals. However, before calculating the mean, the LFP signals are first filtered for ECG-specific frequencies (between 0.5-20 Hz) [36]. Since the noise level of the ECG artefact, stimulation artefacts as well as movement artefacts in the LFP recordings is high, there is a bigger change that most separated components will include some noise. Applying the bandpass filter increases the probability of sufficient isolation of the ECG artefact.

Mathematically, it is impossible to uncover more source signals (independent components) than the number of input signals, so for this approach, only three components are separated. Due to the regularity and salience of the heartbeat, ICA should be able to separate the ECG artefact as one of the first components. The current method uses kurtosis as nongaussianity measure and a fixed-point optimization algorithm to separate the components (FastICA, [37]). To select which component represents the ECG artefact, the components are normalized and applied with the same ECG detection algorithm as previously described (see section 2.4.1). The component specified as ECG artefact is kept, while the other two are set to zero. By performing inverse ICA, the part caused by ECG artefact is isolated from the recorded LFP signals (right panel Fig. 2).

Similar to the template subtraction method, the cleaned LFP signals are then obtained by subtracting the ECG artefact, $LFP_{ECG}(t)$, of the original LFP signals, *LFP(t)*, (4). However, instead of solely suppressing the ECG artefact at the QRS complex epochs, the ICA-based method suppresses the ECG artefact over the entire recording.

$$LFP_{clean}(t) = LFP(t) - LFP_{ECG}(t) \quad (4)$$

2.4.3 Performance ECG Artefact Removal

The performances of the template subtraction and ICA-based ECG artefact removal methods are assessed by comparing them to the performance of the Perceive ECG removal. This comparison is done by evaluating the results in time domain as well as comparing the mean relative PSD.

2.5 Synchronization

The current project explores three methods to synchronize the Percept data with the externally recorded TMSi data. Applying the methods to either the left- or right LFP signal of one patient will suffice to synchronize both channels.

2.5.1 External Tapping

The first method for synchronization is external tapping on the F3 or F4 electrode, so on the forehead. The idea is that tapping will not only cause an artefact on the electrode itself,

but also on the DBS electrode, since the electrode is placed close to the burr hole.

2.5.2 Stimulation Ramping

Another proposed method to synchronize the data recording systems is by slightly ramping the stimulation up and down at the start of the recording. The F3 and F4 electrodes are expected to capture this ramping of stimulation, which can be synchronized with the LFP data of the Percept since the stimulation amplitude is registered while recording the LFPs.

To find the moment F3 and/or F4 captures the stimulation ramping, the rate of change with respect to time is calculated. This is done by taking the derivative of the F3 and/or F4 signal with respect to time (5):

$$\textit{Rate of Change} = d\,(F3) \,/\, d\,(time) \tag{5}$$

The first sample at which the absolute value of the rate of change exceeds a recording-specific threshold, is defined as the start of the stimulation ramping. In order to align the recording systems, the sample at which the stimulation increase is registered by Percept is converted to the sampling frequency of the TMSi. Finally, the TMSi recording is shifted by the difference in samples between the two recording systems.

2.5.3 ECG Cross-Correlation

The last method for synchronization uses cross-correlation to find the delay between the ECG artefact in the LFP signal and the ECG signal measured externally. The cross-correlation is a measure of similarity between two signals as a function of time shift of one relative to the other. Because the ECG artefact is in most cases prominent in the LFP signal of the right hemisphere, that channel is used. A prerequisite for applying cross-correlation is that both signals have the same sampling frequency. Therefore, the ECG signal is first down-sampled to the sampling frequency of the Percept (250 Hz). Both the LFPs as well as the ECG signal are then filtered for ECG-specific frequencies (between 0.5-20 Hz) [36]. After applying the cross-correlation, one signal will be shifted relative to the other such that the peak of similarity will be at a lag of zero and the signals are synchronized.

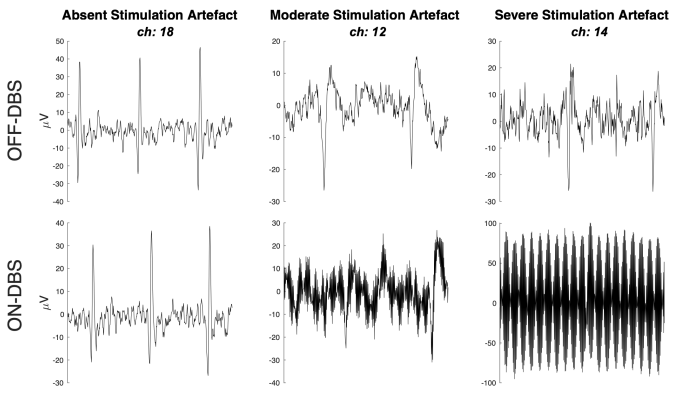

Fig. 3: LFP signals recorded while stimulation was off (upper panels) and on (lower panels). All three channels have severe ECG artefact and are categorized according to the level of stimulation artefact: absent (left), moderate (middle) or severe (right).

2.5.4 Performance Synchronization

In order to rate the performance of the synchronization methods, the LFPs are assessed by cross validation. The synchronization performed by external tapping can be evaluated by proving the stimulation artefact and the QRS complexes in the LFPs overlap with the stimulation artefact captured by the F3 and F4 electrodes and the QRS complex of the externally recorded ECG signal. Likewise, the performance of the synchronization by stimulation artefact can be evaluated by proving the artefact caused by externally tapping and ECG artefact overlap. Finally, the performance of the synchronization by ECG artefact can be evaluated by proving the externally tapping artefact and stimulation artefact overlap.

3 Results

Bilateral recordings of the eleven patients resulted in 22 LFP channels. An overview of these channels is provided in Table 2. Throughout the results, there will be referred to the LFP signals by either calling the individual channel (ch) or both channels of one patient (pt).

3.1 Stimulation Artefact

Despite all measures taken by the manufacturer of the Percept to remove the stimulation artefact (see section 2.2), only five channels had no visual stimulation artefact during the on-DBS condition. The stimulation signal is about one million times larger than the LFP signal, which in most cases leads to an increase in recorded LFP signal amplitude. Furthermore, the stimulation often causes the operational amplifier of the Percept to saturate, which results in a spiky signal as shown in the middle and right panel of Fig. 3.

Table 2. Overview of the recorded LFP channels

Channel	Patient	Side	Sensing Contact Pair	ECG Visible
1	1	L	0 - 2	Minor
2	2	L	0 - 2	Minor
3	3	L	0 - 2	Minor
4	4	L	0 - 2	Minor
5	5	L	0 - 2	Minor
6	6	L	0 - 2	Minor
7	7	L	0 - 2	Severe
8	8	L	0 - 3	Severe
9	9	L	0 - 2	Minor
10	10	L	0 - 2	Moderate
11	11	L	0 - 2	Minor
12	1	R	0 - 2	Severe
13	2	R	0 - 2	Moderate
14	3	R	0 - 2	Severe
15	4	R	1 - 3	Moderate
16	5	R	0 - 2	Minor
17	6	R	1 - 3	Moderate
18	7	R	1 - 3	Severe
19	8	R	1 - 3	Severe
20	9	R	0 - 2	Moderate
21	10	R	1 - 3	Severe
22	11	R	0 - 2	Minor

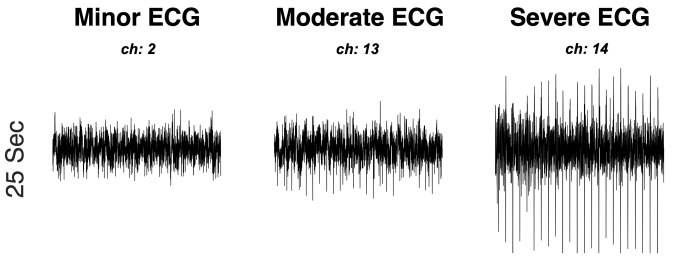

Fig. 4: Examples of the ECG artefact in the time domain. Channels are categorized into minor, moderate and severe ECG contamination.

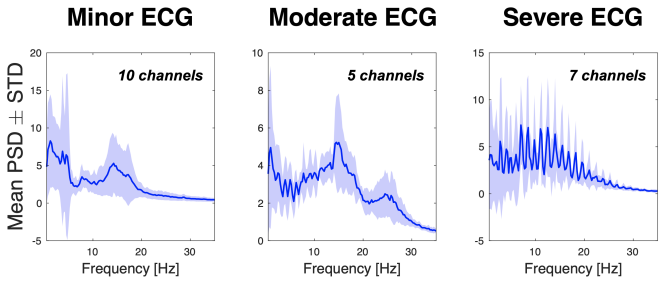

Fig. 6: The mean relative power spectral density (PSD) with the standard deviation (STD). Categorized into minor, moderate and severe ECG contamination.

3.2 ECG Artefact Removal

Considering the stimulation artefact during on-DBS, consistency is assured by applying the ECG artefact removal methods only for the off-DBS condition. Although severe ECG artefact will still (vaguely) show from the channels affected by stimulation artefact, the channels in which the ECG artefact is minor or moderate might be left unnoticed. Additionally, the spiky pattern of the stimulation artefact is sometimes indistinguishable from ECG artefact.

The level of ECG artefact in the channels during the off-DBS condition is defined in the right column of Table 2. This discrimination is based on visual inspection of the ECG contamination of the LFP signal in time domain. As an example, the difference in ECG artefact is visualised in Fig. 4. All channels contained at least a minor ECG artefact. If a channel contains only minor ECG artefact, the tip of the QRS complex lays close to the level of neural activity. In five channels, the ECG artefact was moderate and seven channels were even severely contaminated.

3.2.1 *Template Subtraction*

The first step of removing the ECG artefact using the template subtraction method is detecting the R-peaks in the LFP signal. The ECG detection algorithm successfully detects the R-peaks of channels in which the ECG artefact was moderate and severe (twelve channels in total). The algorithm does not work sufficiently in channels with minor ECG artefact. The mean relative PSD with its standard deviation (STD) in Fig. 6 shows that minor ECG artefact affects the frequency content of the LFPs only mildly. Therefore, the fact that the ECG detection algorithm only works for moderate and severely contaminated channels is acceptable.

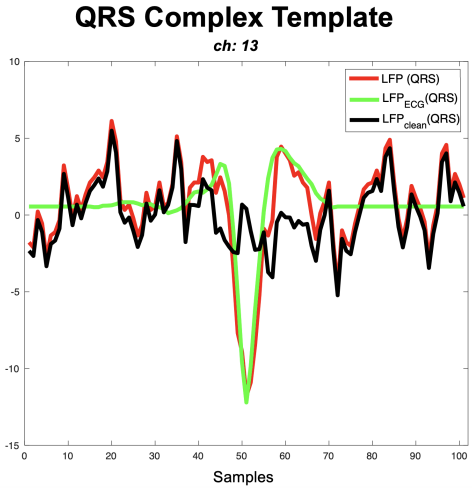

Fig. 5: One epoch of the original LFP signal containing the QRS complex (*LFP (QRS)*, red line); The QRS-specific optimized template ($LFP_{ECG}(QRS)$, green line). Ultimately, this optimized template is subtracted from this particular LFP epoch, resulting in an LFP signal at the QRS complex epoch with artefact removed ($LFP_{clean}(QRS)$, black line).

For each ECG contaminated channel, the ECG artefact template is generated. On each QRS complex epoch, this template is adjusted to optimally subtract the ECG artefact. An example of a QRS complex template specifically optimized for one particular epoch is shown in Fig. 5. The result of the template subtraction for the example channels in which the ECG artefact is moderate and severe is visualized in the upper panels of Fig. 7, respectively.

3.2.2 *Independent Component Analysis*

For the ICA-based method, both channels of one patient are analysed together. Five patients have at least one channel in which the ECG artefact is moderate, and five patients have at least one channel in which the ECG artefact is severe (Table 2).

The most important feature of the ICA-based method, is separating the ECG artefact as one of the three independent components (IC) (Fig. 8). If the ECG detection algorithm assigns all three components as containing ECG artefact, it will basically be a very cumbersome way of applying a 0.5-20 Hz bandpass filter. Similarly, since an ECG component usually is a higher power signal, too much signal content below 20 Hz is also filtered if two of the three components are detected as ECG artefact.

None of the components separated in patients with minor ECG contamination are detected as ECG artefact. The ICA was not capable of separating any ECG component in two of the five patients with moderate ECG contamination. In one patient, two components were detected as ECG artefact. This means that the ICA was only capable of separating one ECG component in two of the five patients that have at least one channel in which the ECG artefact is moderate. In all five patients that have at least one channel with

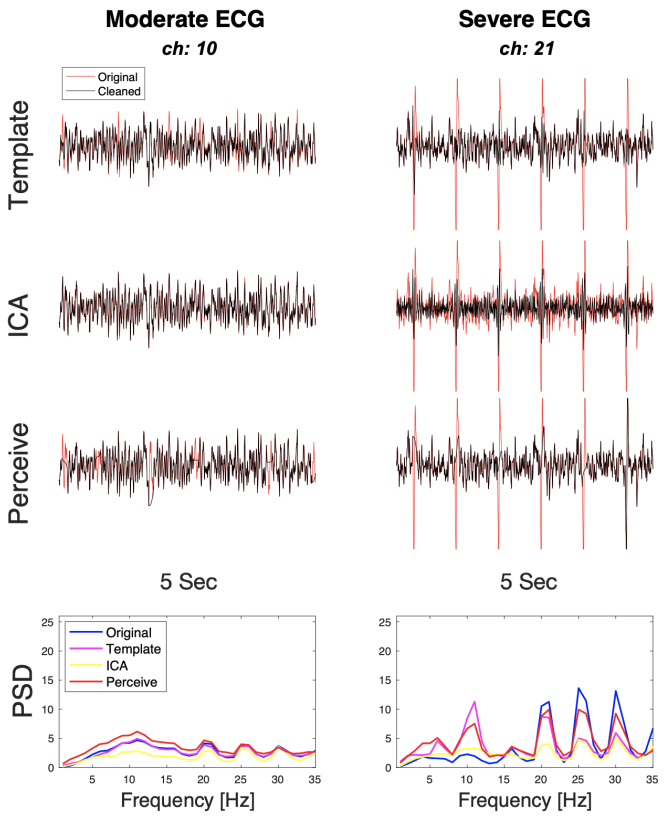

Fig. 7: The result of suppressing moderate and severe ECG artefact (respectively left and right) by template subtraction (upper panels), ICA (second row panels), and Perceive Toolbox (third row panels). The effect of the ECG removal methods on these two channels in frequency domain is shown by the relative PSD in the lower panels.

severe ECG artefact, the ICA was able to separate one ECG component. However, in these patients, ICA sometimes separates two ECG components. That is why the ICA is run repeatedly until it separates only one ECG component, with a maximum of twenty runs.

The result of the ICA-based ECG removal method in time domain is shown in the middle panels of Fig. 7. These channels were recorded from the left- and right hemisphere of patient 10 and had moderate and severe ECG artefact, respectively. Fig. 9 contains a more thorough analysis of the effect of the ICA ECG removal method on these channels. The upper panels of this figure show the LFP signals of the other patient that has one channel in which the ECG artefact is moderate and for which the ICA was capable of separating one single ECG component. For patient 10, the other channel contained severe ECG artefact. Contrarily, the other channel of patient 6 only contains minor ECG artefact. Due to the fact that the ICA-based method uses both channels as input, the level of ECG artefact in the other channel has a massive impact on the result of the ECG removal. This difference in performance suggests that the ICA-based method basically separates the channel with the worst ECG contamination as ECG component and subtracts that share of both channels.

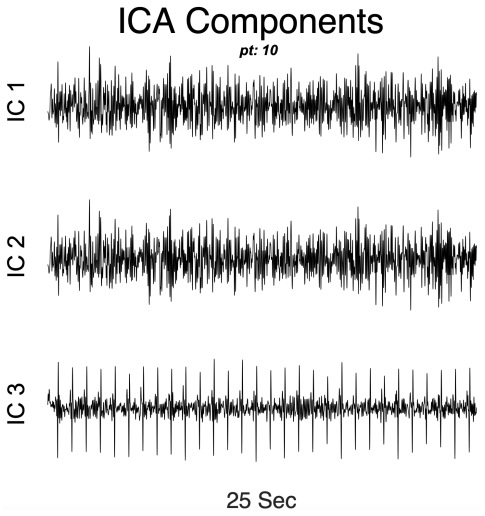

Fig. 8: An example of the independent components (IC) as a result of the FastICA. In this specific case, only the third separated component (IC 3 - lower panel) is detected as ECG artefact contributor.

3.2.3 *Performance ECG Artefact Removal*

The upper three rows of panels in Fig. 7 represent the difference between the ECG removal methods in time domain. Here it shows that for the channel with severe ECG artefact, the template subtraction method effectively suppresses the QRS complexes, whereas the ICA-based method leaves a residue of the R-peaks in the signal. The Perceive Toolbox suppresses the R-peaks sufficiently, though only if the R-peak is correctly detected. When looking at the channel with moderate ECG artefact, it shows that the Perceive method annotates different parts of the signal as R-peaks than the ECG detection algorithm used for the template subtraction method. The fact that the Perceive Toolbox occasionally even misses out on an R-peak in severely contaminated channels suggests that their method of pattern matching of the template on the raw signal is less adequate than the ECG detection algorithm of the template subtraction method.

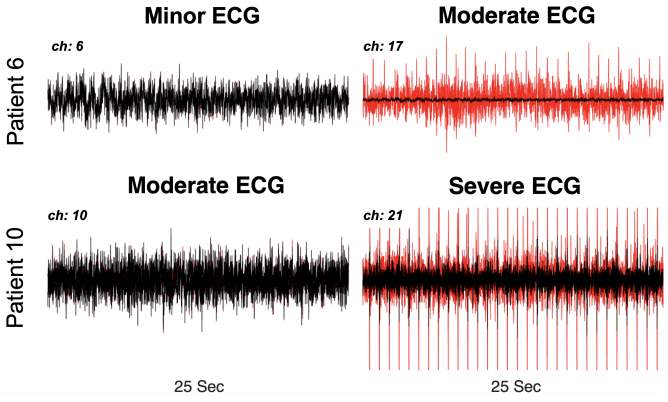

Fig. 9: The result of the ICA-based method in time domain for the two patients that have at least one channel in which the ECG artefact is moderate and for which the ICA was capable to separate one single ECG component. The LFP signals are obtained from the left- and right hemisphere, respectively.

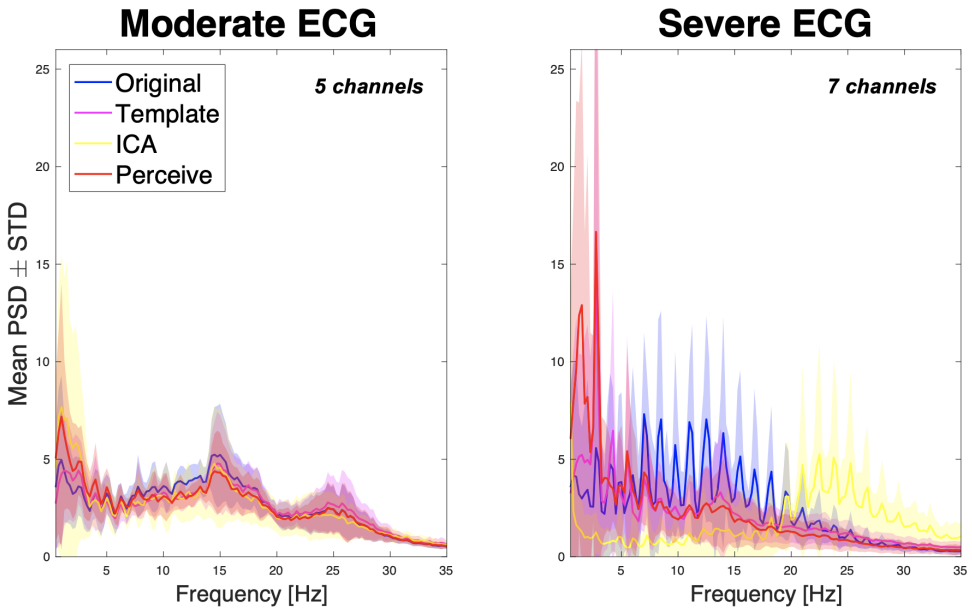

Fig. 10: The performance of the ECG removal methods for moderate and severe ECG artefact contamination.

Next, the performance of the proposed ECG removal methods are compared by evaluating the mean relative PSD (Fig. 10). For moderate ECG artefact, this figure shows that the template subtraction performs best in reducing the spiking pattern of PSD caused by the ECG artefact. Moreover, the proportion power of the lower frequencies reduces most for the template subtraction method. All three methods perform sufficiently in preserving the important beta peak. However, as discussed in section 3.2.2 and Fig. 9, the ICA was only applied to two channels, of which one was basically left unaffected. Therefore, the mean relative PSD result of the ICA is not as meaningful as of the template subtraction and Perceive Toolbox.

The unreliability of the ICA-based method becomes apparent from the result of the severely contaminated LFP signals (right panel of Fig. 10). Here, the power of frequencies below 20 Hz are greatly reduced. The ICA method is designed to isolate the ECG artefact by first applying a 0.5-20 Hz bandpass filter. Usually, the ECG component is of high power. Subtracting this ECG component of the original LFP signal explains why the the relative PSD after ICA ECG suppression shows such a big reduction of power below 20 Hz. Contrarily, both the template subtraction method as well as the Perceive Toolbox ECG removal method perform well on reducing the ECG artefact. As a matter of fact, the beta peak is absent in the relative PSD of the original LFP signal, and becomes apparent after applying the template subtraction method. Similar to the results on the moderate ECG artefact, the template subtraction method shows the highest performance on preserving the beta frequency peak while the proportion of lower frequency power reduces.

3.3 Synchronization

The following sections will discuss the proposed methods to synchronize the Percept data with the externally recorded TMSi data. Again, the results will refer to specific patients instead of separate channels. Contrary to the ECG removal methods, synchronization is performed in both the off-DBS condition, as well as to the on-DBS condition.

3.3.1 *External Tapping*

Tapping on the electrode close to the burr hole (F3 and F4 electrodes) does not cause an artefact on the LFP signals (Fig. 11). Medtronic probably recommended this way of synchronization because they assumed newly implanted patients would be recorded, for which the burrhole is not yet fully recovered. Additionally, tapping does not cause a clear artefact in the signals of the F3 or F4 electrodes when

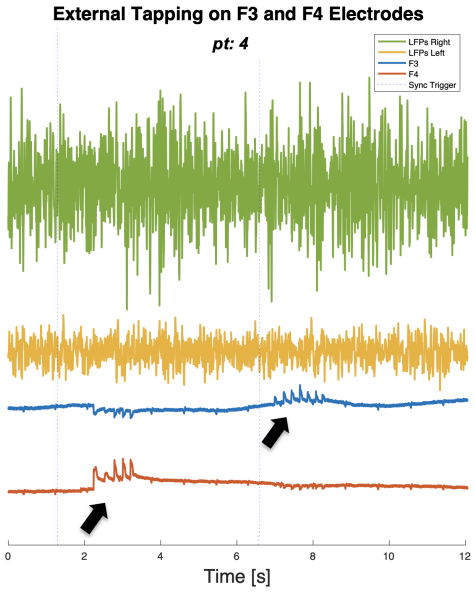

Fig. 11: Normalized LFPs and signals measured at the F3 and F4 electrodes, after synchronization using ECG cross-correlation. The black arrows indicate seven times externally tapping on F3, and five times on F4.

the stimulation is on. That case, the stimulation artefact overshadows the external tapping. As an alternative, we tried tapping with an accelerometer on the skin above the freshly implanted case of the Percept. Apart from this being uncomfortable for the patient due to the sensitivity of the skin immediately after surgery, it did not leave any sign of artefact on the LFPs.

3.3.2 Stimulation Ramping

In the off-DBS condition, the stimulation amplitude was slightly ramped up and down as an attempt to synchronize the recording systems. Apparently, the Percept splits the streamed data into separate recordings when changing either the pulse width or the frequency of the simultaneously delivered stimulation. Ramping up and down the stimulation amplitude does not split the recording. This feature of the Percept should be taken into account when using stimulation ramping to synchronize the data.

Fig. 12 shows the normalized signal of the stimulation amplitude registered by the Percept, as well as the normalized signals captured by the F3 and F4 electrodes. When analyzing critically, the signals at the F3 and F4 electrodes indicate that the stimulation is not yet turned off while the Percept already registers zero stimulation amplitude. Apparently, the Percept only registers the stimulation amplitude twice per second (with 2 Hz). This is far less precise than the stimulation artefact captured by the F3 and F4 electrodes and will reduce the accuracy of the synchronization.

The LFP signals, on the other hand, are recorded at 250 Hz. Despite all the efforts taken by the manufacturer of the Percept to remove the stimulation artefact (see section 2.2), all of the recordings still show an increase of LFP amplitude and/or a step response on the electrode lead of which the stimulation is ramped up or down. By ramping up the stimulation on the left side, the amplitude of the LFP signal of the left hemisphere increases (Fig. 13). An example of the step responses that sometimes occur when ramping the stimulation is shown around 700 seconds in the upper panel of Fig. 14. Due to the higher sampling frequency of the LFPs compared to the registered stimulation amplitude, using the stimulation artefact on the LFPs to synchronize the recording systems is more precise. On the other hand, the stimulation artefact is reflected differently on each sensing channel. Therefore, applying this method of synchronization requires quite a lot of coding.

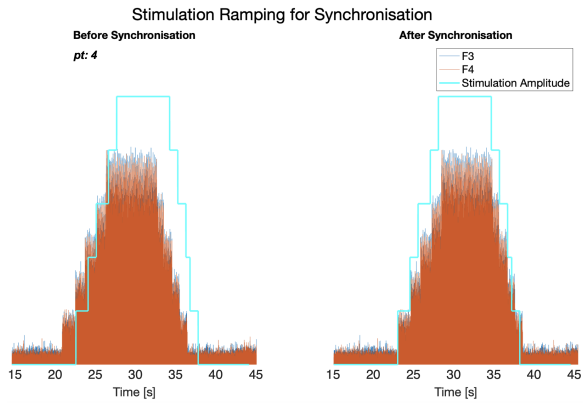

Fig. 12: Stimulation amplitude (at 60 Hz) and the normalized and absolute signals measured at the F3 and F4 electrodes (50 Hz high pass filtered).

3.3.3 ECG Cross-Correlation

The final method proposed to synchronize the recording systems, is by making use of the minor ECG artefact present in every recording with Percept. From Table 2, it is determined that the LFP signal of the right hemisphere is usually the channel with a bigger ECG artefact. The upper panel of Fig. 14 shows the LFPs of the right hemisphere during the full recording (both off- and on-DBS condition) of one patient. The middle panel is the bipolar ECG signal measured between two electrodes placed on the shoulders. The lower panel shows the zoomed in result of the cross-correlation between the upper two signals. The maximum correlation is found at 11960 lag, which corresponds to approximately 48 seconds.

Interestingly, recordings that only have minor ECG artefact still find a clear optimum time lag. Furthermore, the cross-correlation also finds a peak in the on-DBS recordings. However, there is also a potential pitfall of this method. That is, using the LFP signal of the left hemisphere leads to a small difference in optimum time lag. The fact that the externally recorded ECG signal has to be downsampled to 250 Hz before cross-correlation can be performed, might induce these small lateral differences.

3.3.4 Performance synchronization

Although externally tapping on the F3 and F4 electrode or at the case of the Percept seems as a convenient method to cause a clear simultaneous artefact at both

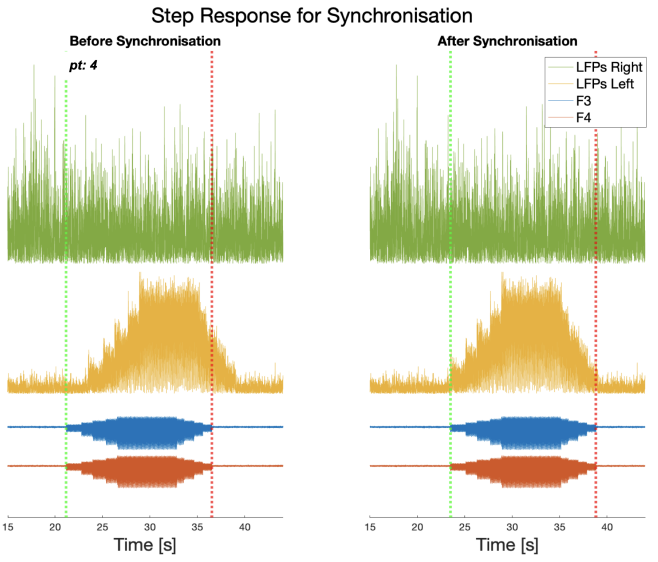

Fig. 13: LFP signals of the left- and right hemisphere (normalized, absolute and 90 Hz high pass filtered) and signals measured at the F3 and F4 electrodes.

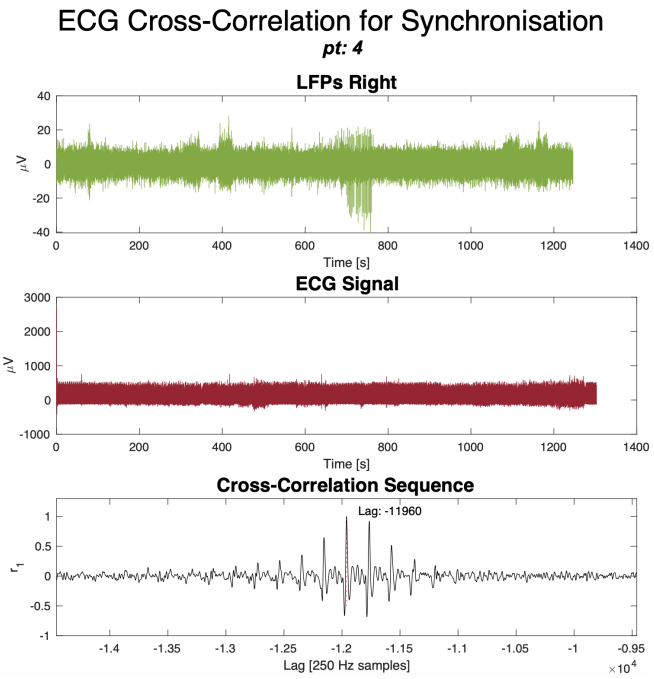

Fig. 14: LFP signal of right STN filtered for ECG-specific frequencies (upper panel); Externally recorded ECG signal filtered for ECG-specific frequencies (middle panel); Cross-correlation coefficient of the LFP- and ECG signal over samples (250 Hz).

recording systems, this was not the case. That means the synchronization can only be cross validated for the stimulation artefact method and the ECG cross-correlation method.

To be able to perform a cross validation, the recording must contain both a stimulation- as well as a ECG artefact. Fig. 15 shows the cross validation of one patient in which both synchronization methods are successful. The upper panels contain the results of synchronization using the stimulation artefact, the lower panels show the result after synchronizing using ECG cross-correlation. In both cases, the stimulation artefact on the LFP signal and on the F3 electrode are aligned, as well as the R-peaks of the ECG artefact on the LFP signal and the externally recorded ECG signal. As expected, the time lag between the LFPs and the ECG signal (filtered for ECG-specific frequencies) after such successful synchronization through stimulation artefact is only minimal (3 samples $\sim$ 12 ms).

The cross validation of the synchronization methods in another patient is shown in Fig. 16. This figure suggests, however, that the ECG cross-correlation method result in an incorrect synchronization. After both synchronization methods, the R-peaks of the ECG artefact align. However, the stimulation artefact proves that the ECG cross-correlation picked up the wrong time lag. It is most likely that the repetitive nature of the ECG artefact caused the cross-correlation to have shifted one heartbeat.

3.4 Proof of Concept for Tasks Analysis

As the LFP signal is synchronized with the TMSi data, the start and stop triggers can be used to cut the recording into the different tasks of the protocol. The relative PSD during rest, the finger-to-nose-test (movement) [38], and reading out loud (speech) before and after ECG artefact suppression are calculated (Fig. 17). Due to missing data, there are no channels with moderate ECG artefact for which the synchronization could be cross-validated that also contain data for all three tasks. All seven channels with severe ECG artefact contain data for the three tasks, though the synchronization of only two could be cross-validated in the off-DBS condition. These were channels 8 and 19; the left and right hemisphere of patient 8.

The upper panels of Fig. 17 show that it is impossible to analyze the differences in relative PSD between the tasks in the original data containing severe ECG artefact. Since the ICA-based method has shown to be unable to suppress the ECG artefact (section 3.2.3), the analysis of cutting the recording

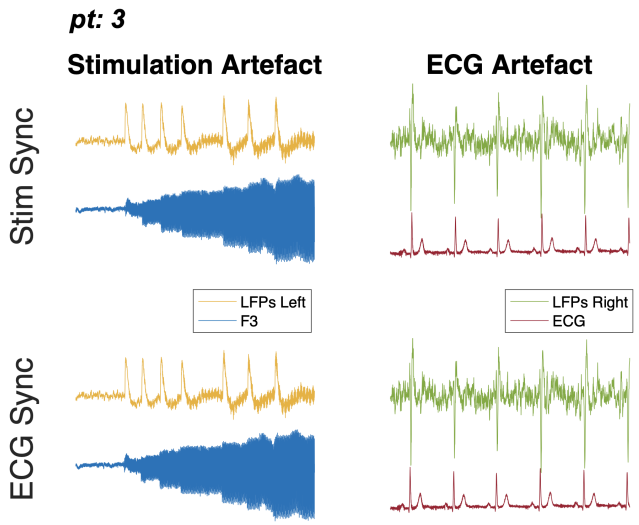

Fig. 15: Cross validation of the synchronization methods. For this recording, both synchronization methods are successful.

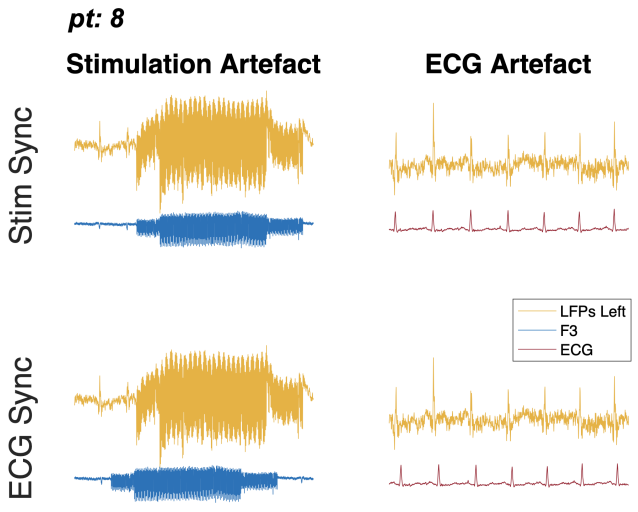

Fig. 16: Cross validation of the synchronization methods. This result suggest that the ECG cross correlation is not successful.

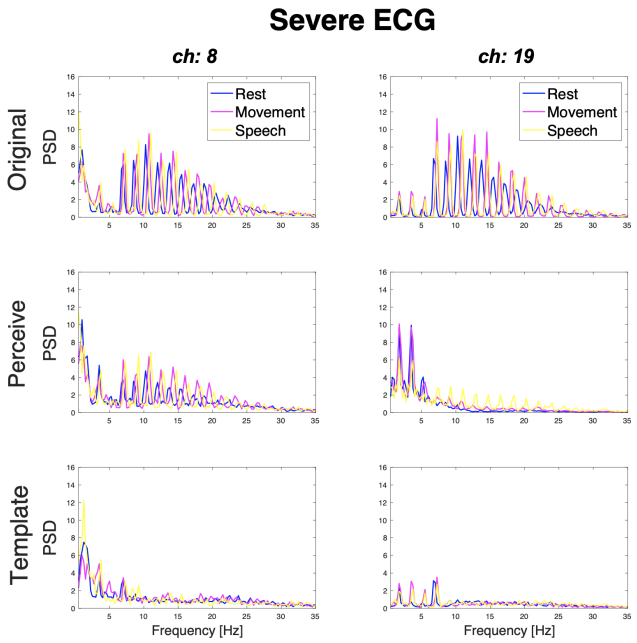

Fig. 17: The relative PSD of channels 8 (left column) and 19 (right column) of the original signal (upper panels), the signal after ECG artefact suppression using the Perceive Toolbox (middle panels), and after the template subtraction method is applied (lower panels). This figure demonstrates the feasibility of the Perceive ECG suppression method and template subtraction method to start analyzing the differences in brain activity during different tasks: rest (61 seconds, blue line), finger-to-nose-test (32 seconds, pink line), and reading out loud (33 seconds, yellow line).

into different tasks is not performed on the LFP signals after applying the ICA-based method. Although the ECG removal method of the Perceive Toolbox seems to perform well on reducing severe ECG artefact of the entire recording (Fig. 10), the middle panels of Fig. 17 demonstrate that it is still not possible to analyze the differences in relative PSD of the LFPs between tasks after applying the Perceive method. However, the lower panels of Fig. 17 prove that suppressing the ECG artefact using the template subtraction method makes it feasible to start analyzing the differences between tasks for individual frequencies. Unfortunately, for patient 8, no clear differences in relative PSD of the LFP signal between the tasks are found.

4 Discussion

The current study explores the sensing capabilities of the Medtronic Percept™, a fully implanted neurostimulator able to simultaneously record LFPs and deliver stimulation. Although this technology paves the way for the development of adaptive DBS, it is difficult to obtain a reliable LFP signal due to ECG contamination. Additionally, adaptive DBS can only be applied if the feedback signal is indicative of the patients' clinical state. Further research that aims to create a patient-specific profile of neuronal activity correlated with the severity of the motor symptoms requires synchronization of the Percept data with externally recorded data.

In this study, two methods for removing ECG artefact were developed: 1) an optimized template subtraction and 2) an ICA-based ECG suppression. These methods were evaluated both in time- as well as in frequency domain. The performances were compared to each other, and to an existing ECG artefact removal method implemented in the open-source Perceive Toolbox. Following these analyses, the optimized template subtraction method performs best in effectively suppressing the QRS complex present in the LFP signal as well as preserving the frequency content.

In order to extract features in the brain signal that correlate with the patients' motor symptoms, the second aim of this study was to find a way to synchronize the LFP signal with externally recorded data. Here, three methods were explored. Externally tapping on an electrode close to the burr hole did not leave an observable artefact on the LFPs, nor did tapping on the neurostimulator. Contrary, both ramping the stimulation as well as using the ECG cross-correlation did allow to synchronize the recording systems.

4.1 Similarities and Differences of the Perceive Toolbox ECG Removal Method and the Template Subtraction Method

As the results of the current study show that the template subtraction method performs better at suppressing the ECG artefact than the ECG removal method implemented in the Perceive Toolbox, it is important to understand their similarities as well as their differences. The two ECG removal methods are similar in that they both aim to detect and suppress the QRS complexes present in the LFP signal. However, the algorithms used by the methods to detect the segments containing the QRS complexes differ. The ECG detection algorithm of the Perceive Toolbox performs pattern matching over the raw signal by a template generated using cross-correlation. The Perceive method will always detect segments that have a matching pattern, but these segments do not necessary have to be actual QRS complexes. The template subtraction method, on the other hand, specifically searches for the R-peaks that meet the criteria described in section 2.4.1. The two methods also differ in how the ECG artefact suppression is performed. The Perceive Toolbox applies mirrored padding over the QRS complexes, whereas the template subtraction method uses a QRS-specific optimized template to suppress the ECG artefact.

4.2 ECG Suppression Preserves Significant Part of Signal's Information

The two ECG artefact removal methods developed in the current study both aim to isolate the ECG artefact from the LFP signal (Fig. 2). The part containing this ECG artefact is then subtracted from the original LFP signal. The fact that the methods suppress the ECG artefact at the significantly affected segments of the LFP signal, instead of removing all these segments, is beneficial for the continuity of the recording. Previous studies to PD have reported that the pathological beta-band activity is not constantly increased but comes in bursts of different durations and amplitudes [10], [39]. Bursts with a longer duration are positively correlated with motor impairment in PD, while bursts of shorter duration are negatively correlated. Cutting out the artefacts

and attaching the rest of the recording or replacing the segments containing artefact with zero would have made burst analysis impossible.

4.3 Improving ECG Detection Algorithm for Better ECG Artefact Removal

Fig. 10 shows that the beta frequency peak reenters most effectively when the ECG artefact is removed by the template subtraction method, as compared to the ICA and Perceive Toolbox. However, template subtraction does only work for LFP signals in which the ECG artefact is moderate or severe. This limitation is due to the performance of the ECG detection algorithm. A suggestion to enable ECG artefact removal using the template subtraction method of LFP signals with minor contamination, is by obtaining the timings of the QRS complexes by applying the ECG detection algorithm to the simultaneous externally recorded ECG signal. This approach, however, will rely heavily on perfect synchronization of the recording systems. A better solution is suggested by Chen and colleagues [40], who demonstrated the feasibility of recording an ECG reference signal using the monopolar montage of a sensing-enabled neurostimulator. That method even allowed to extract a clear R-peak through large stimulation artefacts. In theory, the Percept could be implemented with such ECG reference signal as well, but currently is not. It is noteworthy, however, that the PSD of an LFP signal is only minimally affected by minor ECG artefact. That is why care has to be taken when removing minor ECG artefact, such that unnecessary loss of LFP information is avoided.

4.4 Include Lateral Optimization to Further Improve Template Subtraction Method

The performance of the template subtraction method does not only depend on the performance of the ECG detection algorithm. The current method allows for scaling of the waveform of the ECG artefact. However, characteristics of the ECG artefact, i.e. the shape of the waveform, might alter due to fatigue or discomfort [18]. If the optimization would also allow the QRS complex template to lengthen or shorten in time, the effect of the template subtraction method could even further improve.

4.5 Evaluation of the ICA-based ECG Removal Method

Theoretically, there are many aspects in favor of applying an ICA-based method for ECG artefact removal. ICA makes use of the joint ECG contamination of both hemispheres. Therefore, if one hemisphere only has minor ECG contamination, the ICA should be able to use the same ECG contamination present in the other hemisphere to remove the ECG artefact in both. Secondly, whereas the template subtraction method improves with increasing number of QRS complexes, the performance of an ICA-based method will not increase with a longer recording duration. Theoretically, ICA could also be applied to the recording split into the separate tasks. This could even improve its performance since irregularities of the ECG artefact (caused by, for example, the heart rate) will reduce. However, for the current data sets, cutting the recording into smaller pieces did not improve performance.

Despite the plausible theory behind the ICA-based method, it showed to be incapable of removing the ECG artefact from the LFP signals. Typically, the channel containing the biggest ECG contamination was separated as ECG component and subtracted from both channels. This lead to almost full suppression of frequency content below 20 Hz for the most severely ECG contaminated channel. Apart from its incapability to serve its purpose, another problem with this method was the inconsistency of ICA in separating components. The fact that the components may vary each time the ICA is performed, is because the technique is initialized with a random vector of weights. This inconsistency makes this method unrepeatable.

4.6 The Wavelet-ICA Approach as a Last Attempt

An explanation for the malfunction of the ICA-based method to remove ECG artefact is the fact that ICA is capable of estimating original signals which are non-Gaussian distributed. However, the problem here is that the sources are not known to be Gaussian or non-Gaussian. In addition, the LFP signal is the result of the joint activity of multiple neurons. This actually means that the number of sources is greater than the number of observations, making it impossible for the ICA to separate the source signals [41]. For the current approach, the number of observations are generated by taking the LFP signals from both hemispheres and their mean. However, another proposed method to increase the number of observations in a single channel recording is to precede ICA by wavelet decomposition [35]. Wavelet analysis splits the LFP signal into a number of frequency components. These signals have non-overlapping spectra and could be taken together to serve as multidimensional input for ICA. Although this combined wavelet-ICA approach has shown to successfully remove ECG artefacts from surface EMG recordings [35], it did not allow to remove the ECG artefact from the recorded LFP signals in the current study. This difference in performance could be due to the small range of frequency of interest of the LFPs compared to EMG data.

4.7 The Choice of synchronization Method is a Trade Off Between Effort and Reliability

The results in section 3.3 indicate that externally tapping does not allow synchronization of the isolated Percept data with the TMSi data, as opposed to the stimulation artefact and the ECG cross-correlation methods. Either of the latter two synchronization methods have their advantages and disadvantages. Both methods require the experimental set up to include one or two extra electrodes. However, considering the ECG artefact in the LFPs, it is sensible to measure the ECG signal anyway. The signals at F3 and F4 serve no additional purpose. When using the stimulation artefact, the experimenter should also remember to ramp the stimulation up and down, whereas the ECG cross-correlation does not need any additional actions from the experimenter. This makes the ECG cross-correlation method easier to use for recordings of short duration, as no extra time will be spent on the synchronization. Apart from the

convenience of the ECG cross-correlation method during the patient recording, this method also runs fully automatic at the stage of offline data processing. The stimulation artefact, on the other hand, is reflected differently on each sensing channel and requires a recording-specific threshold. Therefore, applying this method of synchronization requires quite a lot of coding. As shown from the cross validation of the two methods, the trade off for the minimal effort of the ECG cross-correlation method is its reliability. It synchronizes the recording systems without supervision which apparently may lead to an inaccuracy of one heartbeat.

4.8 Current Adaptive DBS Research Aims for Artefact-Free LFP Recordings

Both effective synchronization methods (stimulation artefact and ECG cross-correlation) depend on the induction of an artefact in the LFP signal. However, as the development of neurosensors progresses, manufacturers aim to remove both the stimulation artefact as well as the ECG artefact altogether. Artefacts reduce the signal to noise ratio and therefore the reliability of the LFPs to serve as feedback signal for adaptive DBS. A recent paper by Debarros and colleagues [42] achieved a LFP recording free of stimulation artefacts by synchronizing the sensing sampling clock with the stimulation pulse. That way, the stimulation pulses happen between the sensing samples which means that the stimulation artefacts are never sampled. Other research to adaptive DBS focuses on avoiding or removing ECG artefact. Strategic placement of the IPG is one suggested approach to mitigate ECG contamination [22], [23]. Neumann and colleagues [22] found that the ECG artefact appears to be stronger and more frequent when the IPG is implanted on the left side of the chest, when compared to right or cranial implants. The current study confirms that finding, as the Percept was implanted on the left side of the chest in four out of the seven channels with severe ECG artefact. Another suggestion to eliminate ECG artefact from the LFP signals is by post-hoc ECG removal methods as proposed in the current study. However, even if this proves to be possible in real-time, which is a prerequisite for adaptive DBS, it will involve additional power consumption. Alternative approaches to reduce ECG artefact are improving the electrical properties of the electrode leads and extensions or developing new coatings to lower the impedance of the tissue-electrode interface. Although an artefact-free LFP recording is essential to detect and extract reliable features in the LFP signal, these features are only informative when correlated to the patients' symptom-severity. In order to find such well-established correlations, manufacturers of neurosensors should facilitate the synchronization of the isolated LFP data with externally recorded data.

5 Recommendations

Regarding the ECG artefact in the LFP signal, several suggestions can be made for future research. First of all, ECG artefact should be avoided as much as possible. The site of IPG implantation, among others, seems to have an impact on the level of ECG artefact [22]. Although a right chest/abdomen implant location reduces ECG contamination in LFP signals as compared to left implant locations, the development of DBS systems should focus on cranial mount systems. Whereas the current project focused on the ECG artefacts, another source of LFP contamination are movement artefacts. Cranial mount systems are suggested to allow only minimal physical motion of the lead and IPG, which would minimize movement artefacts as well.

As long as the ECG artefact can not be avoided, there is enough room for improvement of the proposed ECG removal methods. Considering both the template subtraction method as well as the Perceive Toolbox to remove ECG artefact, the externally recorded ECG signal could be used to identify the timings of the QRS complexes. Although this would allow to suppress the ECG artefact in channels with minor contamination as well, its result will depend on perfect synchronization. Research that focuses on the development of a system added with an ECG reference to the monopolar montage, as previously described [40], would be preferred. Another suggestion to further improve the performance of the template subtraction method, is to include lateral optimization of the QRS complex template.

The current study evaluated the level of ECG artefact visually. Objective measurements of the ECG contamination would allow a more reliable validation of the ECG removal methods. Another recommendation for future studies is to apply the ECG removal methods to a simulated LFP signal with ECG artefact. That way, the simulated clean LFP signal is available which allows to quantify the ECG removal performance. Finally, follow-up analysis of the template subtraction method should involve a recommendation of minimum recording duration required to obtain a reliable QRS complex template. The accuracy of the template improves with increasing number of QRS complexes. Therefore, the longer the recording duration, the better the performance of the template subtraction method. However, it is very likely that at some point, the improvement of template accuracy is only minimal. Knowledge of such optimum between the duration of the recording and the accuracy of the QRS complex template can be useful for future recordings of shorter duration.

Some other suggestions for future research regards the synchronization aspect of the current study. Considering its ease of use, it is worth analyzing why the ECG cross-correlation method is not always reliable. One could argue the repetitive nature of the ECG artefact causes the inaccuracy. However, in general, an ECG signal also contains small variability of heart rate or inter-beat interval. The cross-correlation should actually be able to use these irregularities present in both signals to determine the optimum time lag.

In case a true artefact-free LFP recording is achieved, the synchronization methods proposed in the current study cannot be used. An sensible solution for the manufacturers of Percept to secure the accuracy of synchronization is to increase the sampling frequency by which the stimulation amplitude is registered from twice per second to the same

sampling frequency as the LFP signal (250 Hz). Alternatively, an ECG reference signal could be added to the monopolar montage of the sensing-enabled neurostimulator. Apart from being useful to remove the ECG artefact, such ECG reference signal could also be used for the synchronization. Instead of using the ECG artefact in the LFP signal, this ECG reference signal could be cross-correlated with the externally recorded ECG signal.

6 Conclusion

The ICA-based method was incapable of removing the ECG artefact in the LFP signal, whereas the template subtraction method performed even better than the Perceive ECG removal method in suppressing ECG artefact while preserving LFP frequency content. The performance of the template subtraction method could be further improved by 1) implementing lateral optimization of the QRS complex template, and by 2) using the timings of the QRS complexes determined by an externally recorded ECG signal or by an ECG reference signal added to the monopolar montage of a sensing-enabled neurostimulator.

As long as the reason of failure of the ECG cross-correlation method to synchronize the Percept data with the TMSi data is unclear, a compromise between effort and accuracy can be made by applying the ECG cross-correlation method, but validate its performance by confirming accurate alignment of the stimulation artefact. As current research aims for artefact-free LFP recordings, manufacturers of neurosensors should facilitate a way to synchronize the LFP signals with externally recorded data in order to assist research focused on finding a reliable feedback signal for adaptive DBS.

References

[1] A. Lozano and M. Hallett, *Brain stimulation*. Elsevier, 2013.

[2] R. Mehanna and E. C. Lai, "Deep brain stimulation in Parkinson's disease," *Translational Neurodegeneration*, vol. 2, no. 1, p. 22, 2013. [Online]. Available: https://doi.org/10.1186/2047-9158-2-22

[3] A. M. Kuncel and W. M. Grill, "Selection of stimulus parameters for deep brain stimulation," pp. 2431–2441, 11 2004. [Online]. Available: http://www.ncbi.nlm.nih.gov/pubmed/15465430

[4] A. Merola, M. Zibetti, S. Angrisano, L. Rizzi, V. Ricchi, C. A. Artusi, M. Lanotte, M. G. Rizzone, and L. Lopiano, "Parkinson's disease progression at 30 years: a study of subthalamic deep brain-stimulated patients." *Brain : a journal of neurology*, vol. 134, no. Pt 7, pp. 2074–84, 7 2011. [Online]. Available: http://www.ncbi.nlm.nih.gov/pubmed/21666262

[5] A. Højlund, M. V. Petersen, K. S. Sridharan, and K. Østergaard, "Worsening of Verbal Fluency After Deep Brain Stimulation in Parkinson's Disease: A Focused Review," pp. 68–74, 2017.

[6] J. G. Habets, M. Heijmans, M. L. Kuijf, M. L. Janssen, Y. Temel, and P. L. Kubben, "An update on adaptive deep brain stimulation in Parkinson's disease," *Movement Disorders*, vol. 33, no. 12, pp. 1834–1843, 2018.

[7] S. Little and P. Brown, "Debugging Adaptive Deep Brain Stimulation for Parkinson's Disease," *Movement Disorders*, p. mds.27996, 2 2020. [Online]. Available: https://onlinelibrary.wiley.com/doi/abs/10.1002/mds.27996

[8] A. L. Sette, E. Seigneuret, F. Reymond, S. Chabardes, A. Castrioto, B. Boussat, E. Moro, P. François, and V. Fraix, "Battery longevity of neurostimulators in Parkinson disease: A historic cohort study," *Brain Stimulation*, vol. 12, no. 4, pp. 851–857, 7 2019.

[9] S. Little, A. Pogosyan, S. Neal, B. Zavala, L. Zrinzo, M. Hariz, T. Foltynie, P. Limousin, K. Ashkan, J. Fitzgerald, A. L. Green, T. Z. Aziz, and P. Brown, "Adaptive deep brain stimulation in advanced Parkinson disease." *Annals of Neurology*, vol. 74, no. March, pp. 449–457, 2013.

[10] G. Tinkhauser, A. Pogosyan, S. Little, M. Beudel, D. M. Herz, H. Tan, and P. Brown, "The modulatory effect of adaptive deep brain stimulation on beta bursts in Parkinson's disease," *Brain*, vol. 140, no. 4, pp. 1053–1067, 2017.

[11] A. Kühn, A. Kupsch, G.-H. Schneider, and P. Brown, "Reduction in subthalamic 8-35 Hz oscillatory activity correlates with clinical improvement in Parkinson's disease," *European Journal of Neuroscience*, vol. 23, no. 7, pp. 1956–1960, 2006.

[12] N. Ray, N. Jenkinson, S. Wang, P. Holland, J. Brittain, C. Joint, J. Stein, and T. Aziz, "Local field potential beta activity in the subthalamic nucleus of patients with Parkinson's disease is associated with improvements in bradykinesia after dopamine and deep brain stimulation," *Experimental Neurology*, vol. 213, no. 1, pp. 108–113, 2008.

[13] E. M. Foncke, L. J. Bour, J. D. Speelman, J. H. Koelman, and M. A. Tijssen, "Local field potentials and oscillatory activity of the internal globus pallidus in myoclonus-dystonia," *Movement Disorders*, vol. 22, no. 3, pp. 369–376, 2 2007. [Online]. Available: https://research.utwente.nl/en/publications/local-field-potentials-and-oscillatory-activity-of-the-internal-g

[14] A. Kane, W. D. Hutchison, M. Hodaie, A. M. Lozano, and J. O. Dostrovsky, "Enhanced synchronization of thalamic theta band local field potentials in patients with essential tremor," *Experimental Neurology*, vol. 217, no. 1, pp. 171–176, 5 2009. [Online]. Available: https://linkinghub.elsevier.com/retrieve/pii/S0014488609000491

[15] S. Little, M. Beudel, L. Zrinzo, T. Foltynie, P. Limousin, M. Hariz, S. Neal, B. Cheeran, H. Cagnan, J. Gratwicke, T. Z. Aziz, A. Pogosyan, and P. Brown, "Bilateral adaptive deep brain stimulation is effective in Parkinson's disease," *Journal of Neurology, Neurosurgery and Psychiatry*, vol. 87, no. 7, pp. 717–721, 7 2016. [Online]. Available: https://pubmed.ncbi.nlm.nih.gov/26424898/

[16] D. Piña-Fuentes, S. Little, M. Oterdoom, S. Neal, A. Pogosyan, M. A. Tijssen, T. van Laar, P. Brown, J. M. C. van Dijk, and M. Beudel, "Adaptive DBS in a Parkinson's patient with chronically implanted DBS: A proof of principle," pp. 1253–1254, 8 2017.

[17] J. N. Mak, Y. Hu, and K. D. Luk, "An automated ECG-artifact removal method for trunk muscle surface EMG recordings," *Medical Engineering and Physics*, vol. 32, no. 8, pp. 840–848, 10 2010.

[18] C. Marque, C. Bisch, R. Dantas, S. Elayoubi, V. Brosse, and C. Pérot, "Adaptive filtering for ECG rejection from surface EMG recordings," *Journal of Electromyography and Kinesiology*, vol. 15, no. 3, pp. 310–315, 6 2005.

[19] N. W. Willigenburg, A. Daffertshofer, I. Kingma, and J. H. van Dieën, "Removing ECG contamination from EMG recordings: A comparison of ICA-based and other filtering procedures," *Journal of Electromyography and Kinesiology*, vol. 22, no. 3, pp. 485–493, 6 2012.

[20] M. M. Gulizia, G. Casolo, G. Zuin, L. Morichelli, G. Calcagnini, V. Ventimiglia, F. Censi, P. Caldarola, G. Russo, L. Leogrande, and G. Franco Gensini, "ANMCO/AIIC/SIT Consensus Information Document: Definition, precision, and suitability of electrocardiographic signals of electrocardiographs, ergometry, Holter electrocardiogram, telemetry, and bedside monitoring systems," *European Heart Journal, Supplement*, vol. 19, no. Suppl D, pp. D190–D211, 5 2017. [Online]. Available: https://pubmed.ncbi.nlm.nih.gov/28751842/

[21] N. V. Thakor, J. G. Webster, and W. J. Tompkins, "Estimation of QRS Complex Power Spectra for Design of a QRS Filter," *IEEE Transactions on Biomedical Engineering*, vol. BME-31, no. 11, pp. 702–706, 1984.

[22] W.-J. Neumann, M. Memarian Sorkhabi, M. Benjaber, L. K. Feldmann, A. Saryyeva, J. K. Krauss, M. F. Contarino, T. Sieger, R. Jech, G. Tinkhauser, C. Pollo, C. Palmisano, I. U. Isaias, D. Cummins, S. J. Little, P. A. Starr, V. Kokkinos, S. Gerd-Helge, T. Herrington, P. Brown, R. M. Richardson, A. A. Kühn, and T. Denison, "The sensitivity of ECG contamination to surgical implantation site in adaptive closed-loop neurostimulation systems," *bioRxiv*, p. 2021.01.15.426827, 1 2021. [Online]. Available: https://doi.org/10.1101/2021.01.15.426827

[23] M. Memarian Sorkhabi, M. Benjaber, P. Brown, and T. Denison, "Physiological Artefacts and the Implications for Brain-Machine-Interface Design." [Online]. Available: https://doi.org/10.1101/2020.05.22.111609

[24] E. J. Quinn, Z. Blumenfeld, A. Velisar, M. M. Koop, L. A. Shreve, M. H. Trager, B. C. Hill, C. Kilbane, J. M. Henderson, and H. Brontë-Stewart, "Beta oscillations in freely moving Parkinson's subjects are attenuated during deep brain stimulation," *Movement Disorders*, vol. 30, no. 13, pp. 1750–1758, 11 2015.

[25] N. Mahadevan, C. Demanuele, H. Zhang, D. Volfson, B. Ho, M. K. Erb, and S. Patel, "Development of digital biomarkers for resting tremor and bradykinesia using a wrist-worn wearable device," *npj Digital Medicine*, vol. 3, no. 1, pp. 1–12, 12 2020. [Online]. Available: https://doi.org/10.1038/s41746-019-0217-7

[26] H. Tan, J. Debarros, S. He, A. Pogosyan, T. Z. Aziz, Y. Huang, S. Wang, L. Timmermann, V. Visser-Vandewalle, D. J. Pedrosa, A. L. Green, and P. Brown, "Decoding voluntary movements and postural tremor based on thalamic LFPs as a basis for closed-loop stimulation for essential tremor," *Brain Stimulation*, vol. 12, no. 4, pp. 858–867, 7 2019.

[27] R. Oostenveld, P. Fries, E. Maris, and J. M. Schoffelen, "FieldTrip: Open source software for advanced analysis of MEG, EEG, and invasive electrophysiological data," *Computational Intelligence and Neuroscience*, vol. 2011, 2011. [Online]. Available: https://pubmed.ncbi.nlm.nih.gov/21253357/

[28] W. J. Neumann, J. Huebl, C. Brücke, L. Gabriëls, M. Bajbouj, A. Merkl, G. H. Schneider, B. Nuttin, P. Brown, and A. A. Kühn, "Different patterns of local field potentials from limbic DBS targets in patients with major depressive and obsessive compulsive disorder," *Molecular Psychiatry*, vol. 19, no. 11, pp. 1186–1192, 11 2014. [Online]. Available: www.fil.ion.ucl.ac.uk/spm/

[29] M. Beudel, A. Oswal, A. Jha, T. Foltynie, L. Zrinzo, M. Hariz, P. Limousin, and V. Litvak, "Oscillatory Beta Power Correlates With Akinesia-Rigidity in the Parkinsonian Subthalamic Nucleus," *Movement Disorders*, vol. 32, no. 1, pp. 174–175, 1 2017. [Online]. Available: http://doi.wiley.com/10.1002/mds.26860

[30] E. Petersen, J. Sauer, J. Grabhoff, and P. Rostalski, "Removing Cardiac Artifacts from Single-Channel Respiratory Electromyograms," *IEEE Access*, vol. 8, pp. 30 905–30 917, 2020.

[31] S. Tong, A. Bezerianos, J. Paul, Y. Zhu, and N. Thakor, "Removal of ECG interference from the EEG recordings in small animals using independent component analysis," *Journal of Neuroscience Methods*, vol. 108, no. 1, pp. 11–17, 7 2001. [Online]. Available: https://pubmed.ncbi.nlm.nih.gov/11459613/

[32] J. Iriarte, E. Urrestarazu, M. Valencia, M. Alegre, A. Malanda, C. Viteri, and J. Artieda, "Independent component analysis as a tool to eliminate artifacts in EEG: A quantitative study," *Journal of Clinical Neurophysiology*, vol. 20, no. 4, pp. 249–257, 2003. [Online]. Available: https://pubmed.ncbi.nlm.nih.gov/14530738/

[33] F. Rong and J. L. Contreras-Vidal, "Magnetoencephalographic artifact identification and automatic removal based on independent component analysis and categorization approaches," *Journal of Neuroscience Methods*, vol. 157, no. 2, pp. 337–354, 10 2006. [Online]. Available: https://pubmed.ncbi.nlm.nih.gov/16777232/

[34] G. Barbati, C. Porcaro, F. Zappasodi, P. M. Rossini, and F. Tecchio, "Optimization of an independent component analysis approach for artifact identification and removal in magnetoencephalographic signals," *Clinical Neurophysiology*, vol. 115, no. 5, pp. 1220–1232, 5 2004. [Online]. Available: https://pubmed.ncbi.nlm.nih.gov/15066548/

[35] J. Taelman, S. Van Huffel, and A. Spaepen, "Wavelet-independent component analysis to remove electrocardiography contamination in surface electromyography," in *Annual International Conference of the IEEE Engineering in Medicine and Biology - Proceedings*, vol. 2007. Annu Int Conf IEEE Eng Med Biol Soc, 2007, pp. 682–685. [Online]. Available: https://pubmed.ncbi.nlm.nih.gov/18002048/

[36] M. S. Chavan, R. A. Agarwala, and M. D. Uplane, *Suppression of Noise in the ECG Signal using Digital IIR Filter*.

[37] A. Hyvärinen and E. Oja, "Independent component analysis: Algorithms and applications," *Neural Networks*, vol. 13, no. 4-5, pp. 411–430, 2000. [Online]. Available: https://pubmed.ncbi.nlm.nih.gov/10946390/

[38] G. L. Iverson, "Finger to Nose Test," in *Encyclopedia of Clinical Neuropsychology*. Springer New York, 2011, pp. 1051–1051.

[39] M. Deffains, L. Iskhakova, S. Katabi, Z. Israel, and H. Bergman, "Longer β oscillatory episodes reliably identify pathological subthalamic activity in Parkinsonism," *Movement Disorders*, vol. 33, no. 10, pp. 1609–1618, 10 2018. [Online]. Available: https://pubmed.ncbi.nlm.nih.gov/30145811/

[40] Y. Chen, B. Ma, H. Hao, L. L. F. i. neuroscience, and u. 2021, "Removal of Electrocardiogram Artifacts From Local Field Potentials Recorded by Sensing-Enabled Neurostimulator," *ncbi.nlm.nih.gov*. [Online]. Available: https://www.ncbi.nlm.nih.gov/pmc/articles/PMC8071948/

[41] X. Jiang, G. B. Bian, and Z. Tian, "Removal of artifacts from EEG signals: A review," 3 2019. [Online]. Available: /pmc/articles/PMC6427454/ /pmc/articles/PMC6427454/?report=abstract https://www.ncbi.nlm.nih.gov/pmc/articles/PMC6427454/

[42] J. Debarros, L. Gaignon, S. He, A. Pogosyan, M. Benjaber, T. Denison, P. Brown, and H. Tan, "Artefact-free recording of local field potentials with simultaneous stimulation for closed-loop Deep-Brain Stimulation," in *Proceedings of the Annual International Conference of the IEEE Engineering in Medicine and Biology Society, EMBS*, vol. 2020-July. Institute of Electrical and Electronics Engineers Inc., 7 2020, pp. 3367–3370. [Online]. Available: /pmc/articles/PMC7116199/ /pmc/articles/PMC7116199/?report=abstract https://www.ncbi.nlm.nih.gov/pmc/articles/PMC7116199/

Appendices

Longitudinal recordings in patients implanted with DBS electrodes **VISIT 1 STIM OFF**

Patient Identificatie Nummer: | P | D |__|__|__| **Onderzoeker: |__|__|**

Brainsense meting STIM OFF en ON

Instellen BrainSense met gewenste frequenty en pulse width, 0 mA!

Instrueer de patiënt niet te spreken tijdens de meting.

Gebruik "Start" en "Stop" triggers TMSi per taak!

- ☐ 1 minuut rust
- ☐ 30 seconden statisch bewegen (vingers en pols RECHTS in hyperextensie)
- ☐ 10 seconden rust
- ☐ 30 seconden statisch bewegen (vingers en pols LINKS in hyperextensie)
- ☐ 10 seconden rust
- ☐ 30 seconden tappen RECHTS (wijsvinger op duim tappen RECHTS)
- ☐ 10 seconden rust
- ☐ 30 seconden tappen LINKS (wijsvinger op duim tappen LINKS)
- ☐ 10 seconden rust
- ☐ 30 seconden dynamisch bewegen (RECHTERhand open-dicht knijpen)
- ☐ 10 seconden rust
- ☐ 30 seconden dynamisch bewegen (LINKERhand open-dicht knijpen)
- ☐ 10 seconden rust
- ☐ 30 seconden dynamisch bewegen (RECHTERhand pro/supinatie)
- ☐ 10 seconden rust
- ☐ 30 seconden dynamisch bewegen (LINKERhand pro/supinatie)
- ☐ 10 seconden rust
- ☐ 30 seconden intentionele bewegingen (vinger onderzoeker – neus patiënt RECHTS)
- ☐ 10 seconden rust
- ☐ 30 seconden intentionele bewegingen (vinger onderzoeker – neus patiënt LINKS)
- ☐ 10 seconden rust
- ☐ 30 seconden spraak (tekst oplezen)
- ☐ 10 seconden rust
- ☐ 30 seconden stappen op de plaats (indien mogelijk)
- ☐ 10 seconden rust

BrainSense meting en TMSi meting **CONTINUEREN, NIET PAUZEREN!** *Maar let op: max. 30 min streamen.*

Longitudinal recordings in patients implanted with DBS electrodes **VISIT 1**

STIM ON

Patient Identificatie Nummer: | P | D |__|__|__| **Onderzoeker: |__|__|**

Amplitude (mA) langzaam opvoeren per electrode tot aan gewenste effect (of pre-operatief bepaald mA)
Instellingen Percept:

Rechts
mA _____ Frequency _____ Pulse width _____

Links
mA _____ Frequency _____ Pulse width _____

BrainSense meting met stimulatie aan

Instrueer de patiënt niet te spreken tijdens de meting.

Gebruik "Start" en "Stop" triggers TMSi per taak!

- ☐ 1 minuut rust
- ☐ 30 seconden statisch bewegen (vingers en pols RECHTS in hyperextensie)
- ☐ 10 seconden rust
- ☐ 30 seconden statisch bewegen (vingers en pols LINKS in hyperextensie)
- ☐ 10 seconden rust
- ☐ 30 seconden tappen RECHTS (wijsvinger op duim tappen RECHTS)
- ☐ 10 seconden rust
- ☐ 30 seconden tappen LINKS (wijsvinger op duim tappen LINKS)
- ☐ 10 seconden rust
- ☐ 30 seconden dynamisch bewegen (RECHTERhand open-dicht knijpen)
- ☐ 10 seconden rust
- ☐ 30 seconden dynamisch bewegen (LINKERhand open-dicht knijpen)
- ☐ 10 seconden rust
- ☐ 30 seconden dynamisch bewegen (RECHTERhand pro/supinatie)
- ☐ 10 seconden rust
- ☐ 30 seconden dynamisch bewegen (LINKERhand pro/supinatie)
- ☐ 10 seconden rust
- ☐ 30 seconden intentionele bewegingen (vinger onderzoeker – neus patiënt RECHTS)
- ☐ 10 seconden rust
- ☐ 30 seconden intentionele bewegingen (vinger onderzoeker – neus patiënt LINKS)
- ☐ 10 seconden rust
- ☐ 30 seconden spraak (tekst oplezen)
- ☐ 10 seconden rust
- ☐ 30 seconden stappen op de plaats (indien mogelijk)
- ☐ 10 seconden rust

APPENDIX B
SCRIPT: TEMPLATE SUBTRACTION

```
function clean = Template_ECG_Removal(data)

% Template-based ECG-subtraction method

% Steps:
% 1. Detect LFPs containing ECG artefact
% 2. Determine QRS-complexes in the LFP signal
% 3. Take the mean over the complexes to create a QRS-complex template
% 4. Optimize this template by minimizing the summed squared error
% 5. Subtract the optimized template of the original signal to suppress the ECG artefact.

% If ECG artefact is detected, the output are the cleaned LFPs.

fsample = 250;

flag_peak = 0;

noECGTemp = data;
tvec = 1:length(noECGTemp);

LFPecg = data;

% ---- 1. Detect ECG artefact
LFPnorm = normalize(LFPecg);

[Rpeak,locs_Rwave] = findpeaks(LFPnorm,'MinPeakHeight',(2*std(LFPnorm)),...
    'MinPeakDistance',fsample/2);

% Also apply R-peak detection to flipped signal:
LFPecg = -data;

LFPnorm = normalize(LFPecg);

[Speak,locs_Swave] = findpeaks(LFPnorm,'MinPeakHeight',(2*std(LFPnorm)),...
    'MinPeakDistance',fsample/2);

% Determine which way the peaks are highest, corresponding to R-peaks:
if mean(Speak) > mean(Rpeak)
    locs_Rwave = locs_Swave;
    flag_peak = 1;
else
    LFPecg = data;
    LFPnorm = normalize(LFPecg);
end

% If there are no R-peaks detected at all:
if isempty(locs_Rwave)
    disp('LFPs have no obvious R-peaks')
    % If heartbeats are missed: no ECG artefact is detected:
elseif any(diff(locs_Rwave)/fsample > 3)
    disp('LFPs have no R-peak every three seconds')
    % If heart rate is too low:
elseif length(locs_Rwave) < (40/60)*(length(LFPecg)/fsample)
    disp('LFPs have unreliable heart rate (< 40 bpm)')

    % Else: continue with removal
else
```

```
    % Plot ECG detection figure:
    if fig == 1
        figure;
        hold on
        plot(tvec, LFPnorm)
        plot(locs_Rwave, LFPnorm(locs_Rwave),'rv','MarkerFaceColor','r')
        legend('LFPs', 'Detected R-peaks')
        title('LFPs - filter for ECG', 'FontSize', 18)
    end

% ---- 2. Create QRS complex epochs (400 ms ~ 50 samples before and after R-peak)
    locs = locs_Rwave';
    % Determine start and end sample of epoch
    for i = 1:length(locs)
        locs(i, 1:2)=[locs(i)-50, locs(i)+50];
    end
    % Make sure intervals of 101 samples are possible (begin and end of signal)
    if locs(1) <= 0
        locs = locs(2:end,:);
    end
    if locs(end) > length(data)
        locs = locs(1:end-1,:);
    end

    % Create QRS-template of the epochs the original LFP signal:
    meanLFPecgfreqs = zeros(size(locs,1), 101);
    for i = 1:length(locs)
        meanLFPecgfreqs(i,:) = data(locs(i, 1):locs(i, 2));
    end

% ---- 3. Take the mean of all epochs:
    columnMeans = mean(meanLFPecgfreqs, 1);
    columnMeans1 = columnMeans;



    % Equalize start and end tails:
    if flag_peak == 0
        [~,pw] = findpeaks(-columnMeans);
    elseif flag_peak == 1
        [~,pw] = findpeaks(columnMeans);
    end
    low = find(pw<50);
    high = find(pw>50);

    firsthalf = columnMeans1(1:pw(low(end)));
    tri = delaunayn(firsthalf');
    firstzero = dsearchn(firsthalf',tri,0);
    secondhalf = columnMeans1(pw(high(1)):end);
    tri = delaunayn(secondhalf');
    secondzero = (pw(high(1))-1) + dsearchn(secondhalf',tri,0);
    columnMeans(1:firstzero-1) = columnMeans1(firstzero);       % Let tails run smoothly
to smallest value
    columnMeans(secondzero+1:end) = columnMeans1(secondzero);

    % Important that both tails have same value:
    if columnMeans(end) ~= columnMeans(1)
        % Make beginning same value as end
        firsthalf = columnMeans1(firstzero:pw(low(end)));
        tri = delaunayn(firsthalf');
        firstzero1 = dsearchn(firsthalf',tri,columnMeans(end));
        firstzero1 = firstzero+firstzero1-1;
        columnMeans(1:firstzero1) = columnMeans(end);
    end
```

```
    % Now subtract these templates of the LFP signals

% ---- % 4. Optimize this template ~ lsqnonlin

    ymod2 = zeros(length(locs), length(columnMeans));
    for i = 1:length(locs)
        y = meanLFPecgfreqs(i,:);
        t = 1:length(y);

        % Gradient Search Options
        options = optimset('lsqnonlin');
        options = optimoptions(@lsqnonlin,'Algorithm','trust-region-reflective');
        options = optimset('display','off');

        % Initial Guess & Upper & Lower Bounds
        p0 = [2 2];
        lb = [-10 -10];
        ub = [10 10];

        % Error Function *see end of script!
        func = @(p)fune2(p,columnMeans,y);      % gives vector, required for lsqnonlin

        % LSQnonlin
        [parest,J,~,~,output]=lsqnonlin(func,p0,lb,ub,options);

% ---- 5. Subtract the optimized template, in fune2*
        [noECGTemp(locs(i, 1):locs(i, 2)),ymod2(i,:)] = fune2(parest,columnMeans,y);

    end

    clear LFPecg
    flag_peak = 0;

end

clean = noECGTemp;


% *Error Function
function [e, yhat] = fune2(p,u,y)

a = p(1);   % Scale
b = p(2);   % Offset

% Optimized QRS template:
yhat = a * u + b;

% Error is LFP without ECG artefact: measurement - optimized template
e = y - yhat;
```

APPENDIX C
SCRIPT: ICA-BASED REMOVAL

```
function [clean, ECG_components, iteration] = ICA_ECG_Removal(data)

% ICA-based ECG-removal method

% Steps:
% 1. Filter LFP signal for ECG-frequencies
% 2. Obtain the three inputs for ICA (LFPs Left, LFPs Right, Mean LFPs)
% 3. Run fastICA to generate three components
% 4. Determine which component represents the ECG artefact
% 5. Isolate the ECG artefact component
% 6. Perform inverse ICA
% 7. Subtract the isolated ECG artefact part of the LFP signals of both hemispheres from
both original LFP signals

% The function isolates the ECG artefact and subtract this from the original LFP signal

clean = data;

% ---- 1. Filter LFP signal for ECG-frequencies
    cfg = [];
    cfg.hpfilter    = 'yes';
    cfg.hpfreq      = 0.5;
    cfg.lpfilter    = 'yes';
    cfg.lpfreq      = 20;
    dataECG = ft_preprocessing(cfg, data.LFPs{1});

    flag_isolation = 1;
    ECG_components{1} = zeros(1, 3);  % Variable that saves which component is ECG

    fsample = data.LFPs{1}.fsample;

% ---- 2. Obtain the three inputs for ICA
    x1 = dataECG.trial{1}(1,:);   % Left LFPs (ch 1)
    x2 = dataECG.trial{1}(2,:);   % Right LFPs (ch 2)

    if length(x1) > 2*290 % Signal length must be greater than twice the required FIR
                          filter order (RequiredOrder = 290)

        gem = mean([x1; x2]);       % Mean LFPs
        Zmixed = [x1; x2; gem];     % Three ICA inputs

% ---- 3. Run fastICA to generate three components
        rd = 0;         % Counter to limit 20 iterations

        while rd < 20
            [Zfica, W, T, mu] = fastICA(Zmixed,3,'kurtosis',0);  % Generate three
                                                                   components

% ---- 4. Determine which component represents the ECG artefact

            % ICA-component ECG detection algorithm:
            Zfica2 = zeros(size(Zfica,1),size(Zfica,2));    % Variable to save filtered
                                                              components
            for i = 1:size(Zfica,1)
                Zfica1 = normalize(Zfica(i,:));   % Run each component seperately

                % Two STD threshold height of R-peaks at 0.5 sec distance
                [Rpeak,locs_Rwave] = findpeaks(Zfica1,'MinPeakHeight',(2*std(Zfica1)),...
                    'MinPeakDistance',fsample/2);
```

```
                Zfica1 = normalize(-Zfica(i,:));

                [Speak,locs_Swave] = findpeaks(Zfica1,'MinPeakHeight',(2*std(Zfica1)),...
                    'MinPeakDistance',fsample/2);

                if mean(Speak) > mean(Rpeak)
                    locs_Rwave = locs_Swave;
                end

% ---- 5. Isolate the ECG artefact component; set other two to zero

                % Then check if valid ECG (more than 40 bpm) is in there.
                  If so: isolate it
                if length(locs_Rwave) > (40/60)*(length(Zfica)/fsample) &&
all(diff(locs_Rwave)/fsample < 3)
                    Zfica2(i,:) = Zfica(i,:);
                    ECG_components{1}(1,i) = 1;
                else
                    Zfica2(i,:) = 0;
                    ECG_components{1}(1,i) = 0;
                end

            end

            if length(find(ECG_components{1}(1,:) == 1)) ~= 1
                rd = rd + 1;
                disp(['At iteration ' num2str(rd) ' - '
num2str(length(find(ECG_components{1}(1,:) == 1))) ' ECG Components'])
                iteration = rd;
            elseif length(find(ECG_components{1}(1,:) == 1)) == 1
                iteration = rd;
                rd = 20;
            end
        end

        % Stop running fastICA after 20 iterations
        if length(find(ECG_components{1}(1,:) == 1)) ~= 1 && rd == 20
            Zfica2 = Zfica;
            flag_isolation = 0;
        end


% ---- 6. Perform inverse ICA
        Zr2 = (T \ W' * Zfica2) + repmat(mu,1,size(Zfica2,2));

% ---- 7. Subtract the isolated ECG artefact part of the LFP signals of both hemispheres
from both original LFP signals

        for i = 1:2
            if flag_isolation == 1
                clean.LFPs{1}.trial{1}(i,:) = data.LFPs{1}.trial{1}(i,:) - Zr2(i,:);
            end
        end

    end
```

APPENDIX D
SCRIPT: ECG CROSS-CORRELATION

```
function data = ECGxcorrSync(R, Start, Stop, Sync)

% This function synchronizes Percept data with TMSi data by using the ECG cross-
correlation method.

% Steps:
% 1. TMSi data is downsampled to the same sampling frequency of the Percept (250 Hz)
% 2. Percept and TMSi data are filtered for ECG-specific frequencies (0.5 - 20 Hz)
% 3. Cross-correlation finds time lag between the LFP signal and externally recorded ECG
signal
% 4. One signal is shifted relative to the other to complete synchronization

% R: Variable containing both TMSi and LFP data

% Start: Trigger pressed on TMSi Polybench, indicating start of task [sec]
% Stop: Trigger pressed on TMSi Polybench, indicating stop of task [sec]
% Sync: Trigger pressed on TMSi Polybench, indicating sync of task [sec]

% Get sampling frequencies of both systems:
fsLFP   = R.LFPs{1}.fsample;
fsTMSi   = R.TMSi{1}.fsample;

% ---- 1. Downsample TMSi data to 250 (equal to fsample LFPs):
% (FieldTrip Toolbox)
cfg = [];
cfg.resamplefs = fsLFPs;
TMSi250{1} = ft_resampledata(cfg, R.TMSi{1});

% ---- 2. Filter TMSi250 and LFPs for solely the ECG frequencies:
% (FieldTrip Toolbox)
cfg = [];
cfg.hpfilter    = 'yes';
cfg.hpfreq      = 0.5;
cfg.lpfilter    = 'yes';
cfg.lpfreq      = 20;
LFPstemp{1} = ft_preprocessing(cfg, R.LFPs{1});
TMSitemp{1} = ft_preprocessing(cfg, TMSi250{1});

% Create variable to save lag
tr{1}   = 1;

% Percept LFPs Right Hemisphere (ch 2)
Lr = LFPstemp{1}.trial{1}(2, :);

% TMSi ECG Left (ch 1) and Right (ch 2)
Te1 = TMSitemp{1}.trial{1}(1, 1:end-(fsLFP*10));  % End usually shows big artefact
Te2 = TMSitemp{1}.trial{1}(2, 1:end-(fsLFP*10));
Te  = Te1-Te2;              % ECG Left - ECG Right

% ---- 3. Calculate lag with maximum correlation:
[r1, lags1] = xcorr(Lr, Te);
r1 = r1/max(r1);
[m1, i1] = max(abs(r1));
tr{1} = lags1(i1);
% Outcome:  if t = positive, then LFP lags ECG with t amount of samples
%           if t = negative, then ECG lags LFP with t amount of samples

% ---- 4. Shift one signal in relation to the other signal
% (FieldTrip Toolbox)
cfg = [];
```

```
if tr{1} > 0 % LFPs started first, so shift LFPs to match TMSi
    cfg.begsample = tr{1}+1;                            % tr{1} is basically 0, so start
at first sample by +1
    cfg.endsample = length(Lr);
    S.LFPs{1} = ft_redefinetrial(cfg, R.LFPs{1});
    S.TMSi{1} = R.TMSi{1};                              % TMSi remains the original
elseif tr{1} < 0 % TMSi started first, so shift TMSi to match LFPs
    S.LFPs{1} = R.LFPs{1};                              % LFPs remains the original
    cfg.begsample = ((-tr{1}+1)/fsLFP)*fsTMSi;          % Recalculate to keep high
sampling frequency TMSi
    cfg.endsample = length(R.TMSi{1}.trial{1}(2,:));    % Length of original signal with
high sampling frequency
    S.TMSi{1} = ft_redefinetrial(cfg, R.TMSi{1});
    Start{1} = Start{1} + (tr{1}/fsLFP);                % Add delay in seconds to
triggers
    Stop{1} = Stop{1} + (tr{1}/fsLFP);
    Sync{1} = Sync{1} + (tr{1}/fsLFP);
end

% Make sure time vectors start at 0:
S.LFPs{1}.time{1} = S.LFPs{1}.time{1} - S.LFPs{1}.time{1}(1);
S.TMSi{1}.time{1} = S.TMSi{1}.time{1} - S.TMSi{1}.time{1}(1);

% Make LFPs and TMSi data equal size (in seconds):
cfg = [];
if S.TMSi{1}.time{1}(end) > S.LFPs{1}.time{1}(end)
    cfg.begsample = 1;           % Add starting sample as well!
    cfg.endsample = S.LFPs{1}.time{1}(end)*fsTMSi;
    S.TMSi{1} = ft_redefinetrial(cfg, S.TMSi{1});
elseif S.TMSi{1}.time{1}(end) < S.LFPs{1}.time{1}(end)
    cfg.begsample = 1;           % Add starting sample as well!
    cfg.endsample = S.TMSi{1}.time{1}(end)*fsLFP;
    S.LFPs{1} = ft_redefinetrial(cfg, S.LFPs{1});
end

S.Start = Start;
S.Stop = Stop;
S.Sync = Sync;

data = S;
```